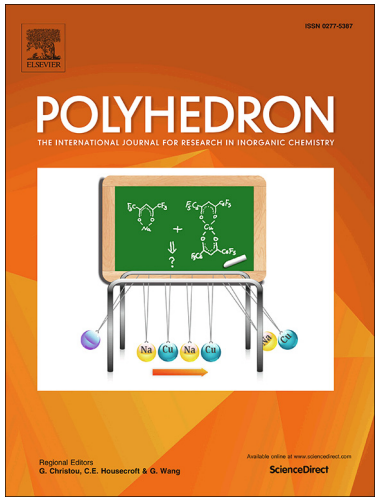

Synthesis, characterization and biological applications of selenoureas having ferrocene and substituted benzoyl functionalities

Raja Azadar Hussain, Amin Badshah, Nadeem Ahmed, John M. Pezzuto, Tammara P. Kondratyuk, Eun-Jung Park, Iqtadar Hussain

PII: S0277-5387(19)30357-2
DOI: https://doi.org/10.1016/j.poly.2019.05.027
Reference: POLY 13952

To appear in: *Polyhedron*

Received Date: 6 April 2019
Revised Date: 11 May 2019
Accepted Date: 13 May 2019

Please cite this article as: R.A. Hussain, A. Badshah, N. Ahmed, J.M. Pezzuto, T.P. Kondratyuk, E-J. Park, I. Hussain, Synthesis, characterization and biological applications of selenoureas having ferrocene and substituted benzoyl functionalities, *Polyhedron* (2019), doi: https://doi.org/10.1016/j.poly.2019.05.027

Synthesis, characterization and biological applications of selenoureas having ferrocene and substituted benzoyl functionalities

Raja Azadar Hussain*[1], Amin Badshah*[1], Nadeem Ahmed[2, 3], John M. Pezzuto[4], Tammara P. Kondratyuk[4], Eun-Jung Park[4], Iqtadar Hussain[5]

1. Co-ordination Chemistry Laboratory, Department of Chemistry, Quaid-i-Azam University, Islamabad (45320), Pakistan.
2. College of Life Sciences, Northwest A & F University, Yangling, Shaanxi, China.
3. Department of Botany, Mohi-ud-Din Islamic University, Nerian Sharif, AJ & K.
4. University of Hawaii at Hilo, United States.
5. Department of Mathematics, Statistics and Physics, Qatar University, Doha (2713), Qatar.

Corresponding Email: hussainazadar@yahoo.com , aminbadshah@yahoo.com , +923009870170

Abstract:

In this article we have comprehensively reported the synthesis, complete chemical characterization (FTIR, multinuclear NMR, single crystal XRD, CHNS, AAS) and biological applications of seventeen ferrocene incorporated selenoureas. Biological applications include comparative DNA binding studies (with, cyclic voltammetry), antioxidant activities (DPPH (2,2-diphenyl-1-picrylhydrazyl) scavenging), anti-inflammatory activities (nitrite inhibition), phase I enzyme inhibition activities (aromatase inhibition), phase II enzyme induction studies (quinone reductase induction) and cytotoxic studies against neuroblastoma (MYCN2 and SK-N-SH), liver

cancer (Hepa 1c1c7) breast cancer (MCF-7) and human cervical carcinoma HeLa cells (ATCC® CCL-2). All the compounds showed decent structure dependent biological applications.

Keywords: Selenourea, ferrocene, enzymology, cytotoxicity, free radicals

1. Introduction

Chemotherapy and radiotherapy are two main routes for treatment of cancer which destroy the cancer cells by apoptosis, mitotic catastrophy, atrophy or terminal growth arrest [1]. However, combination of different methodologies is adopted for treatment of cancer, depending upon the condition of patients, for example in case of advanced stage ovarian cancer (FIGO stage IC-IV), initial debulking surgery is followed by carboplatin-paclitaxel combination chemotherapy. Chemotherapeutic drugs such as melphalan and cyclophosphamide (alkylating agents) doxorubicin and epirubicin (anthracyclines) podophyllin derivatives (etoposide), cisplatin, carboplatin and camptothecins follow a mechanism which is mainly dependent upon the formation of reactive oxygen species (ROS) or free radicals [2]. These free radicals are too much reactive and have the side effects of peripheral neuropathy, nephrotoxicity, ototoxicity, and cardiotoxicity. Therefore it is need of the time to synthesize the drugs which should be more active and less toxic.

Organoselenium derivatives have shown decent activities as anti-infective drugs photochemotherapeutic agents, antitumor agents, cytokine inducers/immunomodulators, antioxidant defense enzymes, enzyme inhibition, antihypertensive and carditonic agents and DNA binders [3-8]. Selenoureas specifically are important enzyme inhibitors, free radical scavengers and anticancer agents [9-11]. Inorganic selenium species (selenium and selenite) are more toxic than organoselenium moieties (selenomethionine and methylseleninic acid) but have

their own importance. So we came up with an idea to synthesize a class of hybrid compounds i.e. organometallic ferrocene incorporated N,N-disubstituted selenoureas which should be active like inorganic selenium species and less toxic like orgaoselenium derivatives [12, 13]. Incorporation of ferrocene into selenourea is important because it is not only a good spectroscopic and electrochemical marker but its presence within the structure of compound has a positive effect on the biological applications of the compound. For example if tamoxifen (active against breast cancer) is incorporated with ferrocene then the development of resistances against it can be reduced with higher activities [14]. In another attempt it has been reported that Illudin M (derived from mushrooms) which is active against prostate, ovarian, pancreatic, renal and breast cancer when connected with ferrocene shows less toxicity for nonmalignant fibroblasts while more cancer selectivity and more cell line specificity than parent Illudin M [15]. Ferrocene incorporated (FI) raloxifens [16], FI nilutamides[17, 18] and FI testosterones [19-22] have shown better results than their parent compounds. Moreover ferrocene is nontoxic and lipophilic which increases the compatibility of the compounds with the cellular media [23]. We have recently reviewed the biological applications of selenoureas [23] and to the best of our knowledge detailed sequential anticancer activities for selenoureas which should start from activities against cancer initiation, proceed through cancer propagation and end up with cancer termination have not been carried out.

In this article we have reported the synthesis of a new class of hybrid (between pure organic and pure inorganic) organometallic compounds in the form of seventeen ferrocene incorporated N,N-disubstituted selenoureas (FIS) and have scanned them for DNA binding studies (with, cyclic voltammetry), antioxidant activities (DPPH (2,2-diphenyl-1-picrylhydrazyl) scavenging), anti-inflammatory activities (nitrite inhibition), phase I enzyme inhibition activities

(aromatase inhibition), phase II enzyme induction studies (quinone reductase induction) and cytotoxic studies against neuroblastoma (MYCN2 and SK-N-SH), liver cancer (Hepa 1c1c7) breast cancer (MCF-7) and human cervical carcinoma HeLa cells (ATCC® CCL-2).

2. Materials and Methods

2.1 General instrumentation

Melting points were determined in a capillary tube using Gallenkamp (U.K) electrothermal melting point apparatus. Infrared spectra were taken on Thermoscientific NICOLET 6700 FTIR between 4000-400 cm^{-1}. ^{1}H and ^{13}C spectra were recorded between 0-13 ppm and 0-210 ppm respectively on Jeol JNM-LA 500 FT-NMR. $Si(CH_3)_4$ was used as internal reference. Elemental analysis was performed using a LECO-932 CHNS analyzer while the Fe concentrations were determined on an Atomic Absorption Spectrophotometer Perkin Elmer 2380.

2.2 DNA binding studies

Commercial salmon DNA was solubalized in doubly distilled water to prepare a stock solution of 5.88 x 10^{-4} M from which working concentrations of DNA were prepared. Concentration of stock solution was measured by UV absorbance at 260 nm using an epsilon value of 6600 $M^{-1}cm^{-1}$. This DNA was protein free because $A_{260}/A_{280} > 1.8$. Working solutions for DNA binding studies were prepared by our previously reported method [6].

2.3 Cyclic voltammetry (CV)

In CV studies a three electrode system was used consisting of working (platinum disc electrode with a geometric area of 0.071 cm^2) reference (Ag/AgCl) and auxiliary electrodes (platinum electrode with geometric area much greater than working electrode). Changes in peak current and peak potential provided the information about drug-DNA binding constant and mode of

interaction respectively. Changes in peak current of the free drug (test compounds in absence of DNA) by the addition of varying concentrations of DNA were used to evaluate the drug-DNA binding constant with the help of following equation [24]:

$$\log (1/[DNA]) = \log K + \log (I/I_{\circ} - I) \quad \text{Eq 1}$$

Where K is the binding constant and $I_{\circ}$ and I are the peak currents of free drug and DNA bound drug respectively.

For the measurement of binding site size (s) following equation was used [25]:

$$C_b/C_f = K[(\text{free base pairs})/s] \quad \text{Eq 2}$$

Where s is the binding site size in terms of base pair, K is the binding constant, C_f is the concentration of free species and C_b represents concentration of drug-DNA bound species. Considering the concentration of DNA in terms of nucleotide phosphate, the concentration of DNA base pair will be taken as [DNA base pair]/2 and Eq 2 will be written as [26]:

$$C_b/C_f = K[(\text{DNA base pair})/2s] \quad \text{Eq 3}$$

The value of C_b/C_f is equal to $(I_{\circ} - I/I)$ which are the values of experimental peak currents.

For the determination of diffusion coefficient of free and DNA bound drug following form of Randles-Sevcik Equation was used [27]:

$$I_{pa} = 2.69 \times 10^5 \, n^{3/2} \, A \, C_{\circ}^{*} \, D_{\circ}^{1/2} \, \upsilon^{1/2} \quad \text{Eq 4}$$

Where I_{pa} is the anodic peak current in ampere, $C_{\circ}^{*}$ is the reductants's concentration in $molcm^{-3}$, υ is the scan rate in $volts^{-1}$, A is the geometric area of the electrode in cm^2, n is the number of

electrons involved in the process and D_o is the diffusion coefficient in cm^2s^{-1}. Same procedure was followed for the interaction of DNA with FIS.

2.4 Free radical scavenging activity

Reducing abilities of all the FIS were determined by monitoring the decrease in the absorbance (with micropipette reader or UV-vis spectrophotometer) at 517 nm of 1,1-diphenylpicrylhydrazyl radical to form 1,1-diphenylpicrylhydrazine. Scavenging activity values were calculated by following equation:

Scavenging activity (%) = A_o-A/A_o x 100 Eq 5

Where A_o is the absorbance of DPPH alone and A is the absorbance of DPPH with different FIS.

2.5 Nitrite inhibition activity

Nitrite inhibition assay was performed according to a previously reported method [28]. According to this method, inside a 96-well plate, 10 x 10^4 cells/plate of RAW 264.7 cells (murine leukemia) were seeded in 10% FBS containing DMEM (Dulbecco's Modified Eagle Medium) for 24 h. Then the media was replaced with 1% FBS-containing (190 µL) phenol red free DMEM and the cultured cells were treated with 10 µL of test samples in 10% DMSO for 15 min. After this step each plate was treated with 1 µgmL^{-1} of LPS for 20 h. Quantitative estimation of nitrite (which is the major oxidation product of NO) was carried out by reacting the incubation media with Griess reagent (90 µL of 1% sulfanilamide in 5% phosphoric acid, and 90 µL of N-(1-Naphthyl)ethylenediamine). Absorbance was scanned at 540 nm according to Eq 5 for percentage inhibition values.

2.6 Aromatase inhibition activity

For aromatase inhibition activity [28], test samples of synthesized compounds were preincubated with NADPH generating system at 37 °C for 10 min. Further incubation for 30 min at 37 °C was carried out before quenching with NaOH after adding the enzyme and substrate to the plates which contained NADPH generating system. Addition of NaOH terminates the reaction and after complete termination the plates were incubated for further 2 h to improve the signal to noise ratio. Fluorescence measurements were carried out at 485 and 530 nm for triplicate readings of five different concentrations of test samples using Letrozole as a positive control.

2.7 Quinone reductase assay

QR (quinone reductase) assay was carried out with hepa 1c1c7 (murine hepatoma) cells which were plated with 200 μL per well with a cell density of 0.5 x 10^4 cells/mL in MEM-α (minimum essential medium) without ribonucleosides or deoxyribonucleosides, supplemented with antimycotic/antibiotic and 10% FBS for 24 h in a carbon dioxide incubator. After 24 h medium was replaced with 190 μL of fresh medium and 10 μL of test samples were added for a final concentration of 4 ppm. After 48 h of incubation, cell membrane was permeabilized with digitonin and enzyme activity was measured by the reduction of 3-(4,5-dimethylthiazo-2-yl)-2,5-diphenyltetrazolium bromide (MTT) to a blue formazan. 4-bromoflavone was used as a positive control and production was measured by absorption at 595 nm [29] with a total protein assay using crystal violet staining run, in parallel [30]. Test samples with an induction ratio > 2 were tested in a 5 fold serial dilutions to determine the CD values [28] .

2.8 Cytotoxic activities

The cytotoxic activities of the test compounds were carried out against neuroblastoma cell lines MYCN and SK-N-SH, hepa 1c1c7 liver carcinoma cell line, human cervical

carcinoma HeLa cells (ATCC® CCL-2) and human breast cancer cell line MCF-7. Briefly, 10 μL of test compounds in all the three series were filled in 96-well plate using 10% DMSO in phosphate buffered saline along with 190 μL of cells (5 x 10^4 cells/mL) and incubated at 37 °C for 72 h in a carbon dioxide incubator. After quenching the incubation with 50 μL of cold 20% trichloroacetic acid, the cells were washed, air dried and stained with 0.4% SRB in 1% acetic acid for 30 min at room temperature. Wells were then washed 4 times with 1% acetic acid solution and plates were dried for 12 h. Bound dye was solubalized in trisbase (200 μL, 10 mM, pH 10) for 10 min on gyratory shaker. For the measurement of optical density at 515 nm, microplate reader (bio-tek) was used which gave information about percent survival. Zero day control was performed in each case with all the procedure mentioned above [28] .

Ferrocene, anilines, sodium nitrite, diethyl ether, acetone, DMSO, Pd-charcoal, carboxylic acid chlorides and hydrazine were purchased from Sigma Aldrich. Ferrocenyl anilines were synthesized by a procedure reported by our group previously [31].

3. Experimental

For the synthesis of FIS, respective carboxylic acid chloride was reacted with potassium selenocyanate in 1:1 using dried acetone as a solvent inside a two necked round bottom flask under constant magnetic stirring. This resulted in the formation of white precipitates of potassium chloride with yellow isoselenocyanate in the solution. The reaction was carried out for 3 h to completion and then 3-methyl-4-ferrocenylphenylaniline was added (1:1 with acid chloride and KSeCN). The reaction took almost 4 h for completion and the progress of reaction was monitored with the help of thin layer chromatography. The resulting orange colored solution was mixed with cold water under constant magnetic stirring. This removed the potassium

chloride suspension and precipitated the product which was then filtered, dried and washed with n-hexane and methanol.

Seventeen new FIS (a1 to a17) were synthesized by the reaction of 3-methyl-4-ferrocenylphenylaniline with different isoselenocyanates according to Scheme 1. 3-methyl-4-ferrocenylphenylaniline was synthesized by using our previously reported procedure [4-7, 23, 32-37]. Structural elucidation of compounds has been given below with structural formula:

3.1 1-acetyl-3-(3-methyl-4-ferrocenylphenyl)selenourea (a1)

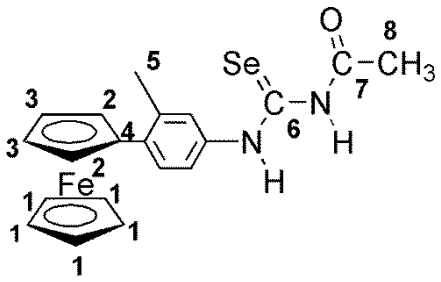

Yield: 69%; **Decomposition temperature:** 136-137 °C; **FT-IR** (cm^{-1}): 3400-3100 (NH stretching broad), 3031 (Aromatic-H stretching), 2956, 2816 (Aliphatic-H stretching), 1659 (C=O stretching), 1573, 1551, 1508 (C=C stretching of aromatic ring), 1382, 1370 (CH_3 bending) 1243 (C=Se stretching); **^{1}H-NMR** (300 MHz, Acetone, δ (ppm): 13.06 (s, 1H, CSeNH), 10.62 (s, 1H, CONH), 8.14-7.30 (m, 3H, Aromatic), 4.73 (apparent t, 2H, *J* 2.1 Hz, ortho on substituted Cp), 4.29 (apparent t, 2H, *J* 1.8 Hz, meta on substituted Cp), 4.11 (s, 5H, Cp-C1), 2.98 (s, 3H, C5), 2.44 (s, 3H, C8); **^{13}C-NMR** (75 MHz, Acetone, δ (ppm): 178.0 (C6), 167.3 (C7), 136.4 (1C-Ar), 135.6 (1C-Ar), 129.3(1C-Ar), 128.7 (1C-Ar), 125.2 (1C-Ar), 112.1 (1C-Ar) 86.3 (C4), 70.0 (C1), 69.4 (C2), 68.2 (C3), 23.1 (C8), 21.1 (C5); **Anal.** Calcd. for $C_{20}H_{20}N_2OFeSe$: C 54.66, N 6.37, H 4.55, Fe 12.75; Found: C 53.43, N 6.21, H 4.51, Fe 12.40%.

3.2 1-benzoyl-3-(3-methyl-4-ferrocenylphenyl)selenourea (a2)

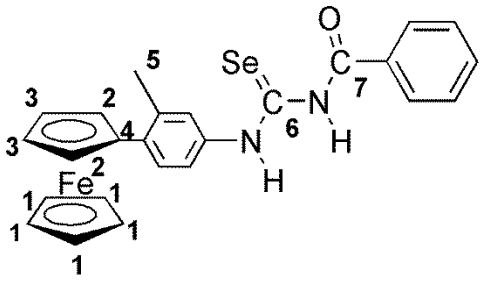

Yield: 63%; **Decomposition temperature:** 134-135 °C; **FT-IR** (cm^{-1}): 3400-3100 (NH stretching broad), 3088 (Aromatic-H stretching), 2921, 2849 (Aliphatic-H stretching) 1667 (C=O stretching), 1584, 1539, 1507 (C=C stretching of aromatic ring), 1361 (CH_3 bending) 1251 (C=Se stretching); **^{1}H-NMR** (300 MHz, Benzene, δ (ppm): 13.41 (s, 1H, CSeNH), 10.50 (s, 1H, CONH), 7.92-6.53 (m, 8H, Aromatic), 4.75 (apparent t, 2H, *J* 2.1 Hz, ortho on substituted Cp), 4.36 (apparent t, 2H, *J* 2.1 Hz, meta on substituted Cp), 4.01 (s, 5H, Cp-C1), 2.44 (s, 3H, C5); **^{13}C-NMR** (75 MHz, Benzene, δ (ppm): 179.0 (C6), 168.6 (C7), 137.5 (1C-Ar), 136.2 (1C-Ar), 133.1 (1C-Ar), 132.0 (1C-Ar), 129.1(1C-Ar), 128.9 (2C-Ar), 126.3 (2C-Ar), 124.4 (1C-Ar), 120.1 (1C-Ar), 112.4 (1C-Ar), 86.4 (C4), 70.0 (C1), 69.7 (C2), 68.5 (C3), 21.5 (C5); **Anal.** Calcd. for $C_{22}H_{22}N_2OFeSe$: C 59.88, N 5.50, H 4.39, Fe 11.11; Found: C 59.01, N 5.39, H 4.27, Fe 10.98%.

3.3 1-(2-bromobenzoyl)-3-(3-methyl-4-ferrocenylphenyl)selenourea (a3)

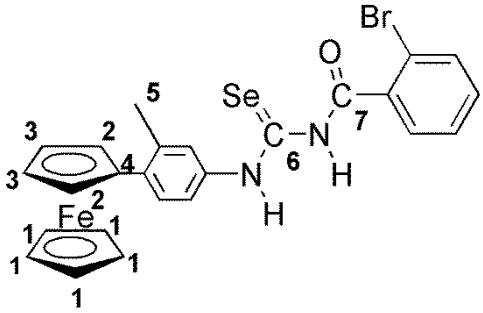

Yield: 62%; **Decomposition temperature:** 163-165 °C; **FT-IR** (cm^{-1}): 3410-3296 (NH stretching broad), 3101 (Aromatic-H stretching), 2929 (Aliphatic-H stretching), 1664 (C=O stretching), 1590, 1552, 1500 (C=C stretching of aromatic ring), 1358 (CH_3 bending), 1245 (C=Se stretching); **^{1}H-NMR** (300 MHz, Acetone, δ (ppm): 13.39 (s, 1H, CSeNH), 9.10 (s, 1H, CONH), 8.15-7.35 (m, 7H, Aromatic), 4.58 (apparent t, 2H, *J* 2.1 Hz, ortho on substituted Cp), 4.33 (apparent t, 2H, *J* 1.8 Hz, meta on substituted Cp), 4.14 (s, 5H, Cp-C1), 2.44 (s, 3H, C5); **^{13}C-NMR** (75 MHz, Acetone, δ (ppm): 177.9 (C6), 164.7 (C7), 145.1 (1C-Ar), 136.7 (1C-Ar), 136.0 (1C-Ar), 133.6 (1C-Ar), 133.1 (1C-Ar), 132.4 (1C-Ar), 131.5 (1C-Ar), 128.6 (1C-Ar) 126.3 (1C-Ar), 126.2 (1C-Ar), 124.0 (1C-Ar), 112.3 (1C-Ar), 86.4 (C4), 69.6 (C1), 69.3 (C2), 68.0 (C3), 21.1 (C5); **Anal.** Calcd. for $C_{25}H_{21}N_2OFeSeBr$: C 51.72, N 4.82, H 3.62, Fe 9.65; Found: C 51.31, N 4.19, H 3.28, Fe 9.09%.

3.4 1-(3-bromobenzoyl)-3-(3-methyl-4-ferrocenylphenyl)selenourea (a4)

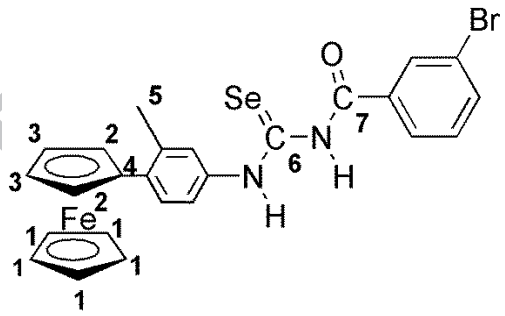

Yield: 67%; **Decomposition temperature:** 172-173 °C; **FT-IR** (cm^{-1}): 3417-3312 (NH stretching broad), 3091 (Aromatic-H stretching), 2948 (Aliphatic-H stretching), 1660 (C=O stretching), 1586, 1557, 1510 (C=C stretching of aromatic ring), 1370 (CH_3 bending), 1244 (C=Se stretching); **^{1}H-NMR** (300 MHz, DMSO, δ (ppm): 12.91 (s, 1H, CSeNH), 9.60 (s, 1H, CONH), 8.44-7.14 (m, 7H, Aromatic), 4.58 (s, 2H, broad, ortho on substituted Cp), 4.33 (s, 2H, broad, meta on substituted Cp), 4.16 (s, 5H, Cp-C1), 2.45 (s, 3H, C5); **^{13}C-NMR** (75 MHz,

DMSO, δ (ppm): 175.9 (C6), 164.7 (C7), 145.0 (1C-Ar), 136.2 (1C-Ar), 135.4 (1C-Ar), 133.1 (1C-Ar), 133.0 (1C-Ar), 132.8 (1C-Ar), 131.5 (1C-Ar), 127.1 (1C-Ar), 126.0 (1C-Ar), 125.6 (1C-Ar), 124.0 (1C-Ar), 112.1 (1C-Ar), 85.1 (C4), 69.1 (C1), 69.0 (C2), 66.0 (C3), 20.9 (C5); **Anal.** Calcd. for $C_{25}H_{21}N_2OFeSeBr$: C 51.72, N 4.82, H 3.62, Fe 9.65; Found: C 51.09, N 4.63, H 3.58, Fe 9.48%.

3.5 1-(4-bromobenzoyl)-3-(3-methyl-4-ferrocenylphenyl)selenourea (a5)

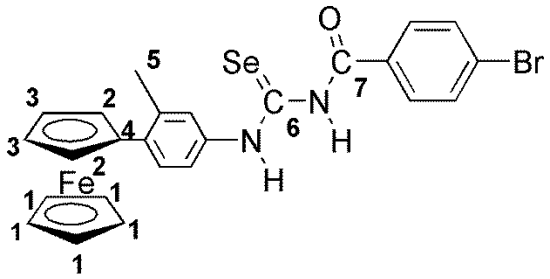

Yield: 53%; **Decomposition temperature:** 189-190 °C; **FT-IR** (cm^{-1}): 3400-3200 (NH stretching broad), 3061 (Aromatic-H stretching), 2938 (Aliphatic-H stretching), 1663 (C=O stretching), 1576, 1561, 1490 (C=C stretching of aromatic ring), 1375 (CH_3 bending), 1256 (C=Se stretching); **^{1}H-NMR** (300 MHz, Acetone, δ (ppm): 13.21 (s, 1H, CSeNH), 10.60 (s, 1H, CONH), 8.20-7.00 (m, 7H, Aromatic), 4.63 (apparent t, 2H, *J* 2.1, ortho on substituted Cp), 4.33 (apparent t, 2H, *J* 1.8, meta on substituted Cp), 4.07 (s, 5H, Cp-C1), 2.46 (s, 3H, C5); **^{13}C-NMR** (75 MHz, Acetone, δ (ppm): 177.9 (C6), 166.2 (C7), 144.3 (1C-Ar), 136.1 (1C-Ar), 135.0 (1C-Ar), 133.4 (1C-Ar), 132.8 (2C-Ar), 131.5 (2C-Ar), 126.3 (1C-Ar), 125.4 (1C-Ar), 124.1 (1C-Ar), 112.9 (1C-Ar), 85.2 (C4), 69.9 (C1), 69.1 (C2), 68.3 (C3), 20.8 (C5); **Anal.** Calcd. for $C_{25}H_{21}N_2OFeSeBr$: C 51.72, N 4.82, H 3.62, Fe 9.65; Found: C 51.69, N 4.59, H 3.41, Fe 9.37%.

3.6 1-(2-fluorobenzoyl)-3-(3-methyl-4-ferrocenylphenyl)selenourea (a6)

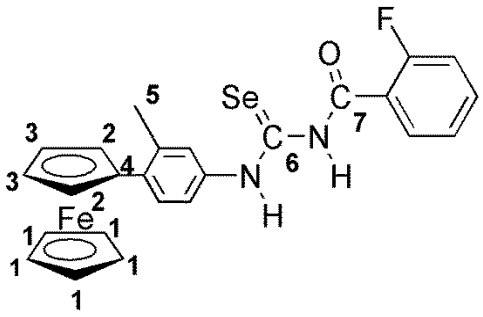

Yield: 78%; **Decomposition temperature:** 154-155 °C; **FT-IR** (cm^{-1}): 3410-3296 (NH stretching broad), 3101 (Aromatic-H stretching), 2929 (Aliphatic-H stretching), 1664 (C=O stretching), 1590, 1552, 1500 (C=C stretching of aromatic ring), 1358 (CH_3 bending), 1245 (C=Se stretching); **^{1}H-NMR** (300 MHz, Benzene, δ (ppm): 13.41 (s, 1H, CSeNH), 9.15 (s, 1H, CONH), 8.80-6.54 (m, 7H, Aromatic), 4.49 (apparent t, 2H, *J* 2.1 Hz, ortho on substituted Cp), 4.44 (apparent t, 2H, *J* 1.8 Hz, meta on substituted Cp), 4.10 (s, 5H, Cp-C1), 2.41 (s, 3H, C5); **^{13}C-NMR** (75 MHz, Benzene, δ (ppm): 178.5 (C6), 168.2 (C7), 158.6 (1C(F)-Ar), 136.9 (1C-Ar), 136.5 (1C-Ar), 135.3 (1C-Ar), 133.6 (1C-Ar), 132.2 (1C-Ar), 130.8 (1C-Ar), 130.4 (1C-Ar), 130.0 (1C-Ar), 129.8 (1C-Ar), 129.6 (1C-Ar), 112.3 (1C-Ar), 87.0 (C4), 69.9 (C1), 69.7 (C2), 68.1 (C3), 21.4 (C5); **Anal.** Calcd. for $C_{25}H_{21}N_2OFeSeF$: C 57.83, N 5.39, H 4.04, Fe 10.75; Found: C 57.82, N 5.37, H 3.98, Fe 10.72%.

3.7 1-(3-fluorobenzoyl)-3-(3-methyl-4-ferrocenylphenyl)selenourea (a7)

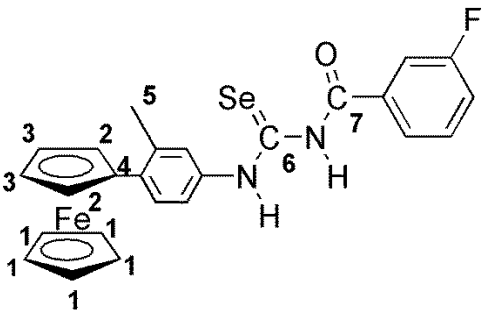

Yield: 61%; **Decomposition temperature:** 149-150 °C; **FT-IR** (cm^{-1}): 3400-3100 (NH stretching broad), 3029 (Aromatic-H stretching), 2953, 2929 (Aliphatic-H stretching), 1657 (C=O stretching), 1561, 1541, 1499 (C=C stretching of aromatic ring), 1377 (CH_3 bending), 1250 (C=Se stretching); **^{1}H-NMR** (300 MHz, Benzene, δ (ppm): 13.40 (s, 1H, CSeNH), 9.08 (s, 1H, CONH), 8.80-6.54 (m, 7H, Aromatic), 4.45 (apparent t, 2H, *J* 2.1 Hz, ortho on substituted Cp), 4.41 (apparent t, 2H, *J* 1.8 Hz, meta on substituted Cp), 4.12 (s, 5H,Cp-C1), 2.44 (s, 3H, C5); **^{13}C-NMR** (75 MHz, Benzene, δ (ppm): 178.3 (C6), 166.3 (C7), 161.0 (1C(F)-Ar), 136.7 (1C-Ar), 136.6 (1C-Ar), 136.5 (1C-Ar), 134.8 (1C-Ar), 133.1 (1C-Ar), 131.7 (1C-Ar), 130.5 (1C-Ar) 130.0 (1C-Ar), 129.6 (1C-Ar), 129.5 (1C-Ar), 112.5 (1C-Ar), 87.4 (C4), 69.1 (C1), 68.7 (C2), 68.1 (C3), 21.3 (C5); **Anal.** Calcd. for $C_{25}H_{21}N_2OFeSeF$: C 57.83, N 5.39, H 4.04, Fe 10.75; Found: C 57.79, N 5.36, H 4.01, Fe 10.70%.[7]

3.8 1-(4-fluorobenzoyl)-3-(3-methyl-4-ferrocenylphenyl)selenourea (a8)

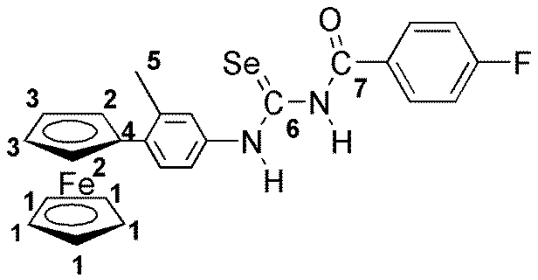

Yield: 74%; **Decomposition temperature:** 165-166 °C; **FT-IR** (cm^{-1}): 3400-3100 (NH stretching broad), 3045 (Aromatic-H stretching), 2951, 2933 (Aliphatic-H stretching), 1663 (C=O stretching), 1569, 1545, 1497 (C=C stretching of aromatic ring), 1377 (CH_3 bending), 1250 (C=Se stretching); **^{1}H-NMR** (300 MHz, Benzene, δ (ppm): 13.41 (s, 1H, CSeNH), 9.13 (s, 1H, CONH), 8.80-6.54 (m, 7H, Aromatic), 4.48 (apparent t, 2H, *J* 2.1 Hz, ortho on substituted Cp), 4.43 (apparent t, 2H, *J* 2.1 Hz, meta on substituted Cp), 4.10 (s, 5H, C1), 2.40 (s, 3H, C5); **^{13}C-NMR** (75 MHz, Benzene, δ (ppm): 178.5 (C6), 166.3 (C7), 158.2 (1C(F)-Ar), 136.9 (1C-

Ar), 136.5 (1C-Ar), 136.3 (1C-Ar), 133.8 (1C-Ar), 132.1 (1C-Ar), 130.9 (1C-Ar), 130.0 (2C-Ar), 129.9 (2C-Ar), 112.5 (1C-Ar), 87.4 (C4), 69.1 (C1), 68.7 (C2), 68.1 (C2), 21.3 (C5); **Anal.** Calcd. for $C_{25}H_{21}N_2OFeSeF$: C 57.83, N 5.39, H 4.04, Fe 10.75; Found: C 57.80, N 5.37, H 4.00, Fe 10.74%.[7]

3.9 1-(2-methoxybenzoyl)-3-(3-methyl-4-ferrocenylphenyl)selenourea (a9)

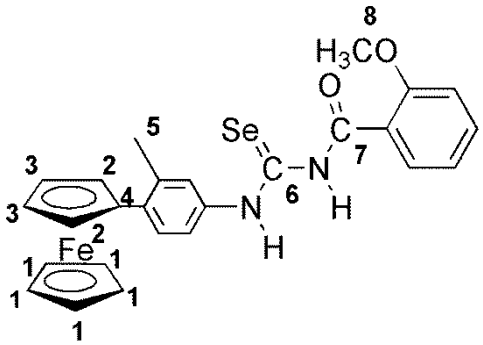

Yield: 49%; **Decomposition temperature:** 181-182 °C; **FT-IR** (cm^{-1}): 3400-3200 (NH stretching broad), 3090 (Aromatic-H stretching), 2944, 2928 (Aliphatic-H stretching), 1659 (C=O stretching), 1599, 1572, 1501 (C=C stretching of aromatic ring), 1363, 1357 (CH_3 bending), 1266 (C=Se stretching); **^{1}H-NMR** (300 MHz, Benzene, δ (ppm): 13.33 (s, 1H, CSeNH), 9.05 (s, 1H, CONH), 8.02-6.03 (m, 7H, Aromatic), 4.83 (apparent t, 2H, *J* 2.1 Hz, ortho on substituted Cp), 4.36 (apparent t, 2H, *J* 1.8 Hz, meta on substituted Cp), 4.10 (s, 5H, Cp-C1), 3.21 (s, 3H, C8), 2.41 (s, 3H, C5); **^{13}C-NMR** (75 MHz, Benzene, δ (ppm): 178.4 (C6), 167.3 (C7), 137.1 (1C-Ar), 136.2 (1C-Ar), 135.0 (1C-Ar), 132.6 (1C-Ar), 132.0 (1C-Ar), 130.0 (1C-Ar), 129.9 (1C-Ar), 129.8 (1C-Ar), 129.7 (1C-Ar), 129.6 (1C-Ar), 119.1 (1C-Ar), 116.2 (1C-Ar), 84.0 (C4), 69.8 (C1), 69.7 (C2), 67.1 (C3), 53.1 (C8), 20.3 (C5); **Anal.** Calcd. for $C_{26}H_{24}N_2O_2FeSe$: C 58.75, N 5.27, H 4.51, Fe 10.54; Found: C 57.98, N 5.20, H 4.40, Fe 10.52%.

3.10 1-(3-methoxybenzoyl)-3-(3-methyl-4-ferrocenylphenyl)selenourea (a10)

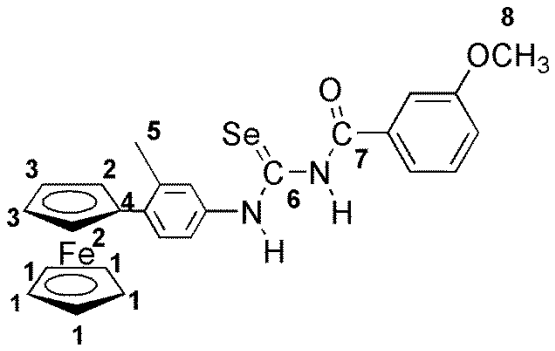

Yield: 55%; **Decomposition temperature:** 170-712 °C; **FT-IR** (cm^{-1}): 3400-3200 (NH stretching broad), 3040 (Aromatic-H stretching), 2941, 2921 (Aliphatic-H stretching), 1670 (C=O stretching), 1588, 1571, 1500 (C=C stretching of aromatic ring), 1359, 1351 (CH_3 bending), 1257 (C=Se stretching); **^{1}H-NMR** (300 MHz, Benzene, δ (ppm): 13.13 (s, 1H, CSeNH), 9.07 (s, 1H, CONH), 8.31-6.59 (m, 7H, Aromatic), 4.81 (apparent t, 2H, *J* 2.1 Hz, ortho on substituted Cp), 4.41 (apparent t, 2H, *J* 2.1 Hz, meta on substituted Cp), 4.15 (s, 5H, Cp-C1), 3.40 (s, 3H, C8), 2.40 (s, 3H, C5); **^{13}C-NMR** (75 MHz, Benzene, δ (ppm): 177.6 (C6), 164.3 (C7), 137.4 (1C-Ar), 135.2 (1C-Ar), 135.0 (1C-Ar), 132.0 (1C-Ar), 131.8 (1C-Ar), 130.0 (1C-Ar), 129.7 (1C-Ar), 129.4 (1C-Ar), 128.9 (1C-Ar), 128.6 (1C-Ar), 118.9 (1C-Ar), 116.4 (1C-Ar), 84.2 (C4), 69.7 (C1), 69.6 (C2), 67.0 (C3), 53.0 (C8), 20.6 (C5); **Anal.** Calcd. for $C_{26}H_{24}N_2O_2FeSe$: C 58.75, N 5.27, H 4.51, Fe 10.54; Found: C 57.23, N 5.16, H 4.40, Fe 10.42%.

3.11 1-(4-methoxybenzoyl)-3-(3-methyl-4-ferrocenylphenyl)selenourea (a11)

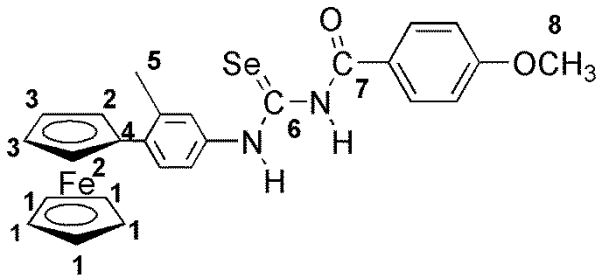

Yield: 53%; **Decomposition temperature:** 156-157 °C; **FT-IR** (cm^{-1}): 3400-3200 (NH stretching broad), 3085 (Aromatic-H stretching), 2967, 2923 (Aliphatic-H stretching), 1645 (C=O stretching), 1600, 1571, 1506 (C=C stretching of aromatic ring), 1379, 1361 (CH_3 bending), 1229 (C=Se stretching); **^{1}H-NMR** (300 MHz, Benzene, δ (ppm): 13.03 (s, 1H, CSeNH), 9.54 (s, 1H, CONH), 8.43-6.33 (m, 7H, Aromatic), 4.73 (apparent t, 2H, *J* 2.1 Hz, ortho on substituted Cp), 4.33 (apparent t, 2H, *J* 1.8 Hz, meta on substituted Cp), 4.00 (s, 5H, Cp-C1), 3.45 (s, 3H, C8), 2.41 (s, 3H, C5); **^{13}C-NMR** (75 MHz, Benzene, δ (ppm): 178.4 (C6), 167.0 (C7), 136.9 (1C-Ar), 135.0 (1C-Ar), 132.0 (1C-Ar), 130.0 (1C-Ar), 129.8 (1C-Ar), 129.5 (1C-Ar), 128.7 (2C-Ar), 128.6 (2C-Ar), 116.4 (1C-Ar), 115.3 (1C-Ar), 84.0 (C4), 69.6 (C1), 69.0 (C2), 68.1 (C3), 54.2 (C8), 20.1 (C5); **Anal.** Calcd. for $C_{26}H_{24}N_2O_2FeSe$: C 58.75, N 5.27, H 4.51, Fe 10.54; Found: C 57.30, N 5.20, H 4.30, Fe 10.05%.

3.12 1-(2-methylbenzoyl)-3-(3-methyl-4-ferrocenylphenyl)selenourea (a12)

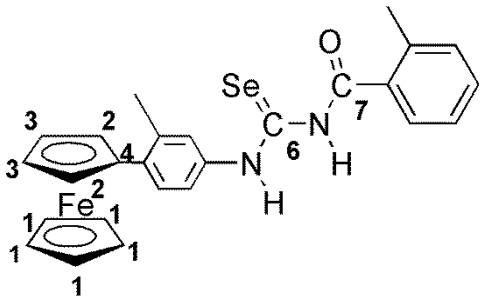

Yield: 73%; **Decomposition temperature:** 146-147 °C; **FT-IR** (cm^{-1}): 3400-3200 (NH stretching broad), 3037 (Aromatic-H stretching), 2936 (Aliphatic-H stretching), 1657 (C=O stretching), 1582, 1544, 1500 (C=C stretching of aromatic ring), 1375 (CH_3 bending), 1264 (C=Se stretching); **^{1}H-NMR** (300 MHz, Benzene, δ (ppm): 12.95 (s, 1H, CSeNH), 9.99 (s, 1H, CONH), 8.42-7.64 (m, 7H, Aromatic), 4.77 (apparent t, 2H, *J* 2.1 Hz, ortho on substituted Cp), 4.29 (apparent t, 2H, *J* 2.1 Hz, meta on substituted Cp), 4.08 (s, 5H, Cp-C1), 2.46 (s, 3H, CH_3), 2.43 (s, 3H, CH_3); **^{13}C-NMR** (75 MHz, Benzene, δ (ppm): 179.3 (C6), 167.4 (C7), 144.3 (1C-

Ar), 136.5 (1C-Ar), 136.1 (1C-Ar), 135.1 (1C-Ar), 132.4 (1C-Ar), 132.1 (1C-Ar), 130.0 (1C-Ar), 129.9 (1C-Ar), 129.7 (1C-Ar), 128.7 (1C-Ar), 128.6 (1C-Ar), 86.5 (C4), 69.6 (C1), 69.7 (C2), 67.7 (C3), 20.7 (1C), 20.3 (1C); **Anal.** Calcd. for $C_{26}H_{24}N_2OFeSe$: C 60.58, N 5.43, H 4.66, Fe 10.87; Found: C 60.50, N 5.30, H 4.32, Fe 10.39%.

3.13 1-(3-methylbenzoyl)-3-(3-methyl-4-ferrocenylphenyl)selenourea (a13)

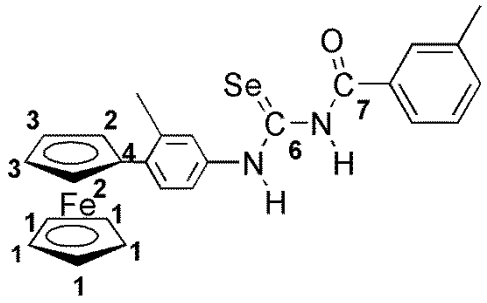

Yield: 68%; **Decomposition temperature:** 143-144 °C; **FT-IR** (cm^{-1}): 3400-3100 (NH stretching broad), 3039 (Aromatic-H stretching), 2939, 2932 (Aliphatic-H stretching), 1668 (C=O stretching), 1582, 1543, 1498 (C=C stretching of aromatic ring), 1371, 1360 (CH_3 bending), 1265 (C=Se stretching); **^{1}H-NMR** (300 MHz, Benzene, δ (ppm): 13.41 (s, 1H, CSeNH), 10.02 (s, 1H, CONH), 8.39-7.09 (m, 7H, Aromatic), 4.76 (apparent t, 2H, *J* 2.1 Hz, ortho on substituted Cp), 4.26 (apparent t, 2H, *J* 2.1 Hz, meta on substituted Cp), 4.18 (s, 5H, Cp-C1), 2.46 (s, 3H, CH_3), 2.45 (s, 3H, CH_3); **^{13}C-NMR** (75 MHz, Benzene, δ (ppm): 179.5 (C6), 166.3 (C7), 143.2 (1C-Ar), 136.3 (1C-Ar), 136.0 (1C-Ar), 135.1 (1C-Ar), 132.0 (1C-Ar), 131.1 (1C-Ar), 130.0 (1C-Ar), 129.6 (1C-Ar), 129.5 (1C-Ar), 128.6 (1C-Ar), 128.5 (1C-Ar), 121.3 (1C-Ar), 86.3 (C4), 69.5 (C1), 69.4 (C2), 67.0 (C3), 20.6 (1C), 20.2 (1C); **Anal.** Calcd. for $C_{26}H_{24}N_2OFeSe$: C 60.58, N 5.43, H 4.66, Fe 10.87; Found: C 60.43, N 5.39, H 4.31, Fe 10.46%.

3.14 1-(4-methylbenzoyl)-3-(3-methyl-4-ferrocenylphenyl)selenourea (a14)

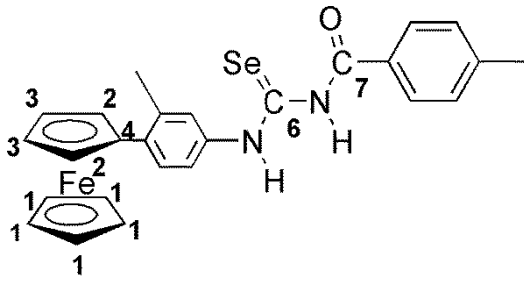

Yield: 79%; **Decomposition temperature:** 155-157 °C; **FT-IR** (cm^{-1}): 3400-3200 (NH stretching broad), 3041 (Aromatic-H stretching), 2939, 2929 (Aliphatic-H stretching), 1660 (C=O stretching), 1592, 1543, 1499 (C=C stretching of aromatic ring), 1371, 1365 (CH_3 bending), 1244 (C=Se stretching); **^{1}H-NMR** (300 MHz, Benzene, δ (ppm): 13.28 (s, 1H, CSeNH), 10.34 (s, 1H, CONH), 8.02-7.42 (m, 7H, Aromatic), 4.60 (apparent t, 2H, *J* 2.1 Hz, ortho on substituted Cp), 4.36 (apparent t, 2H, *J* 2.1 Hz, meta on substituted Cp), 4.17 (s, 5H, Cp-C1), 2.46 (s, 3H, CH_3), 2.44 (s, 3H, CH_3); **^{13}C-NMR** (75 MHz, Benzene, δ (ppm): 179.5 (C6), 167.7 (C7), 144.5 (1C-Ar), 136.0 (1C-Ar), 130.5 (1C-Ar), 129.4 (1C-Ar), 129.3 (1C-Ar), 129.0 (1C-Ar), 128.3 (2C-Ar), 127.4 (2C-Ar), 125.6 (1C-Ar), 121.2 (1C-Ar), 86.5 (C4), 69.6 (C1), 69.3 (C2), 69.2 (C3), 20.7 (1C), 20.5 (1C); **Anal.** Calcd. for $C_{26}H_{24}N_2OFeSe$: C 60.58, N 5.43, H 4.66, Fe 10.87; Found: C 60.51, N 5.38, H 4.29, Fe 10.61%.

3.15 1-(2-chlorobenzoyl)-3-(3-methyl-4-ferrocenylphenyl)selenourea (a15)

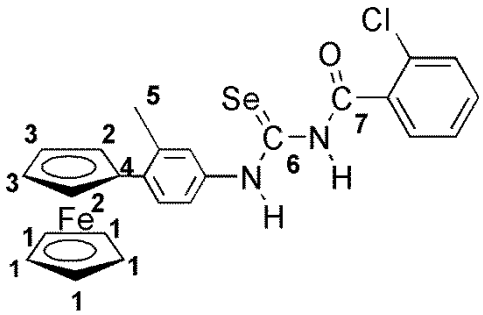

Yield: 63%; **Decomposition temperature:** 167-169 °C; **FT-IR** (cm^{-1}): 3420-3390 (NH stretching broad), 3066 (Aromatic-H stretching), 1659 (C=O stretching), 1599, 1544, 1508 (C=C

stretching of aromatic ring), 1369 (CH_3 bending), 1257 (C=Se stretching); **^{1}H-NMR** (300 MHz, Acetone, δ (ppm): 13.60 (s, 1H, CSeNH), 10.32 (s, 1H, CONH), 8.01-7.10 (m, 7H, Aromatic), 4.65 (apparent t, 2H, *J* 2.1 Hz, ortho on substituted Cp), 4.30 (apparent t, 2H, *J* 2.1 Hz, meta on substituted Cp), 4.07 (s, 5H, Cp-C1), 2.43 (s, 3H, C5); **^{13}C-NMR** (75 MHz, Acetone, δ (ppm): 179.9 (C6), 167.5 (C7), 136.9 (1C-Ar), 136.5 (1C-Ar), 134.1 (1C-Ar), 133.6 (1C-Ar), 133.4 (1C-Ar), 133.1 (1C-Ar), 132.4 (1C-Ar), 126.9 (1C-Ar), 126.0 (1C-Ar), 123.4 (1C-Ar), 120.2 (1C-Ar). 118.6 (1C-Ar), 85.7 (C4), 70.1 (C1), 69.9 (C2), 68.5 (C3), 21.1 (C5); **Anal.** Calcd. for $C_{25}H_{21}N_2OFeSeCl$: C 56.02, N 5.22, H 3.92, Fe 10.45; Found: C 55.67, N 5.11, H 3.74, Fe 10.31%.

3.16 1-(3-chlorobenzoyl)-3-(3-methyl-4-ferrocenylphenyl)selenourea (a16)

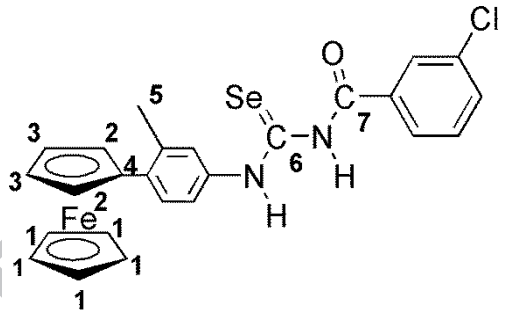

Yield: 67%; **Decomposition temperature:** 177-178 °C; **FT-IR** (cm^{-1}): 3400-3300 (NH stretching broad), 3065 (Aromatic-H stretching), 1658 (C=O stretching), 1598, 1546, 1507 (C=C stretching of aromatic ring), 1368 (CH_3 bending), 1257 (C=Se stretching); **^{1}H-NMR** (300 MHz, Acetone, δ (ppm): 13.60 (s, 1H, CSeNH), 10.30 (s, 1H, CONH), 8.11-7.16 (m, 7H, Aromatic), 4.64 (apparent t, 2H, *J* 2.1 Hz, ortho on substituted Cp), 4.36 (apparent t, 2H, *J* 1.8 Hz, meta on substituted Cp), 4.06 (s, 5H, Cp-C1), 2.43 (s, 3H, C5); **^{13}C-NMR** (75 MHz, Acetone, δ (ppm): 179.8 (C6), 166.4 (C7), 136.9 (1C-Ar), 136.4 (1C-Ar), 134.0 (1C-Ar), 133.5 (1C-Ar), 133.4 (1C-Ar), 133.0 (1C-Ar), 132.1 (1C-Ar), 126.5 (1C-Ar), 126.0 (1C-Ar), 123.1 (1C-Ar), 120.1 (1C-Ar).

119.9 (1C-Ar), 85.6 (C4), 69.9 (C1), 69.7 (C2), 66.9 (C3), 21.3 (C5); **Anal.** Calcd. for $C_{25}H_{21}N_2OFeSeCl$: C 56.02, N 5.22, H 3.92, Fe 10.45; Found: C 55.77, N 5.18, H 3.22, Fe 10.02%.

3.17 1-(4-chlorobenzoyl)-3-(3-methyl-4-ferrocenylphenyl)selenourea (a17)

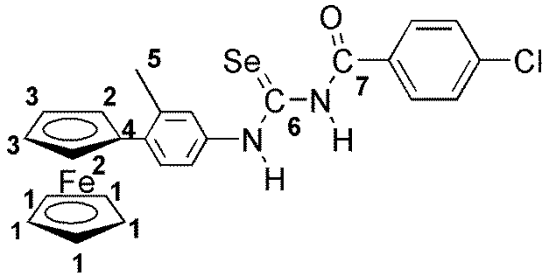

Yield: 77%; **Decomposition temperature:** 182-184 °C; **FT-IR** (cm^{-1}): 3400-3300 (NH stretching broad), 3061 (Aromatic-H stretching), 1661 (C=O stretching), 1597, 1546, 1506 (C=C stretching of aromatic ring), 1371 (CH_3 bending), 1256 (C=Se stretching); **^{1}H-NMR** (300 MHz, Acetone, δ (ppm): 13.60 (s, 1H, CSeNH), 9.91 (s, 1H, CONH), 8.10-7.19 (m, 7H, Aromatic), 4.66 (apparent t, 2H, *J* 2.1 Hz, ortho on substituted Cp), 4.33 (apparent t, 2H, *J* 1.8 Hz, meta on substituted Cp), 4.17 (s, 5H, Cp-C1), 2.44 (s, 3H, C5); **^{13}C-NMR** (75 MHz, Acetone, δ (ppm): 179.7 (C6), 166.0 (C7), 136.8 (1C-Ar), 136.3 (1C-Ar), 133.5 (1C-Ar), 133.3 (1C-Ar), 132.0 (1C-Ar), 128.5 (2C-Ar), 126.9 (2C-Ar), 123.4 (1C-Ar), 120.6 (1C-Ar). 120.0 (1C-Ar), 85.6 (C4), 69.9 (C1), 69.4 (C2), 66.8 (C3), 20.9 (C5); **Anal.** Calcd. for $C_{25}H_{21}N_2OFeSeCl$: C 56.02, N 5.22, H 3.92, Fe 10.45; Found: C 55.39, N 5.10, H 3.81, Fe 10.33%.

4. Results and Discussion

All the FIS were synthesized in good yield having solid state and orange color. In FTIR, -C=Se in all the FIS provided a weak band between 1229-1265 cm^{-1} whereas $–CH_3$ bending vibration was available at ~ 1360 cm^{-1}. Carbonyl stretch in all the synthesized FIS was available above

1650 cm^{-1} whereas –NH stretchings were present above 3200 cm^{-1} as a broad signal. In proton NMR (Figure S-1, supplementary information) the characteristic signals for –NH protons were available above 9 ppm for all the compounds in a way that the –NH proton which was between the phenyl ring attached with ferrocene and –C=Se was comparatively more downfield than the –NH proton which was present between –C=Se and –C=O. The reason may be the intramolecular hydrogen bonding between the oxygen of carbonyl and –NH proton which was present between the phenyl ring and –C=Se. This intramolecular hydrogen bonding was evident in the crystal structure of the representative compound in the series (Figure 1). Unsubstituted cycopentadienyl (Cp) ring yields a singlet at ~ 4 ppm whereas the two protons which are ortho on substituted Cp ring provide a signal which appears as an apparent triplet due to two equivalent protons on meta position. Similarly two protons which are meta on substituted Cp ring provide a signal which appears as an apparent triplets due to two equivalent protons on ortho position with a coupling constant value of ~ 2 Hz. Methyl group present on the phenyl ring (which is attached with ferrocene) gives a singlet for its three protons in all the compounds at ~ 2 ppm. In C-13 NMR (Figure S2, supplementary materials), maximum downfield carbon in all the compounds was the carbon attached with selenium which appeared at ~ 178 ppm whereas carbonyl carbon in all the synthesized FIS was available at ~ 165 ppm. Aromatic carbons were available between 120-140 ppm which is their usual region whereas five carbons of substituted Cp ring provided a singlet and unsubstituted Cp ring gave three peaks in which ipso carbon appeared at ~ 84 ppm due to electron withdrawing effect of phenyl ring with which it is attached. Methyl and metoxy protons whenever available gave their signals at ~ 20 ppm and ~ 51 ppm respectively. Calculated and found percentages of carbon, hydrogen, nitrogen and iron are in close agreement with each other which confirms the purity of the synthesized compounds [34].

4.1 Carcinogenesis

Cancer is the unmanaged growth of cells which may be initiated by the change in genetic makeup or DNA repair mechanism, propagated by further growing of these cells which have wrong growth information to lead the final stage of carcinogenesis which is called tumor. Best chemopreventive agent (CP) will be the one which is active against all the three stages and for that one of the preliminary requirements is that it should bind or interact with DNA. Depending upon the structure and functional groups available on the compounds they can interact via noncovalent and covalent interactions with DNA. Covalent binding is irreversible i.e. it causes complete inhibition of the cellular processes. Alkylating agents and intrastrand linkers generally exhibit covalent interactions with DNA. Noncovalent interactions may be characterized as groove binding, intercalation and external binding. Different techniques are used for the evaluation of DNA binding capabilities of certain possible drugs but we have used cyclic volammetry (CV).

4.1.1 DNA binding studies

DNA binding studies were carried out with the help of CV, mainly because of the best electrochemical signals of ferrocene attached with selenoureas of all the synthesized compounds. DNA binding studies of a representative FIS namely 1-(2-methylbenzoyl)-3-(3-methyl-4-ferrocenylphenyl)selenourea (a12) has been presented in Figure 2. This representative compound gives a couple of well defined redox peaks in a region between 0.6 V to 0.8 V in a diffusion controlled 100% reversible electrochemical process. Reversibility of the process is confirmed by observing three facts i) the difference between oxidation maxima and reduction maxima is almost equal to 60 mV, ii) amplitude of the oxidation peak current and reduction peak current is

~1 and iii) values of current at different scan rates is constant (Figure 2a)) [6]. There is a negative shift in the peak potential of a12-1DNA relative to free a12 which indicates the electrostatic interaction between the phosphate backbone of the DNA and ferrocenium moiety of a12. Because of this electrostatic interaction electrons become available to a12 from DNA which make its oxidation easy and as a result different DNA adducts with a12 provide their oxidation and reduction maxima towards the negative potential side relative to those peaks which are available for free a12 (Figure 2b). Diffusion coefficients were calculated with the help of Eq 4 by a plot of current vs. scan rate. Free a12 has a diffusion coefficient of 1.34 x 10^{-6} cm^2s^{-1} whereas a12-1DNA adduct has a diffusion coefficient value of 4.86 x 10^{-7} cm^2s^{-1} and the same phenomena were true for all the other compounds reported in this article. Lower diffusion coefficients of drug-DNA adducts relative to free drugs confirm the formation of adducts between the drugs and DNA which are of higher molecular weight than free drugs. This increased molecular weight hinders the swift approach of adducts towards the electrode and hence reduces the magnitude of diffusion coefficients. Drug-DNA binding constant of 3.283 x 10^5 M^{-1} was calculated for a12 by using Eq 1. A lower value of the binding site size (0.44 base pair) is also in favor of electrostatic interactions. Drug-DNA binding parameters for all the other compounds have been presented in Table 1 which show that mostly the binding constants are in the range of 10^3-10^5 M^{-1} which are better than DNA binding constants of simple ferrocene [26], nitrophenyl ferrocene [27], ferrocene incorporated thioureas (FIT) [37, 38] and cis-platin. However surface electrostatic interactions generally have inferior binding magnitudes than the universal intercalators ethidium [39] and proflavin [40]. These results gave us very good preliminary information about the possibility of using these FIS as anticancer agents. Our previous findings with molecular docking prove the electrostatic interaction of ferrocenyl moiety

with oxygen (located at DC3 and DG2) of phosphate backbone whereas oxygen of carbonyl group has a tendency to form hydrogen bonds with nitrogenous base pairs [4]. We expect the same behavior of all the FIS presented in this article. If we compare the DNA binding behavior of FIS presented in Table 1 with literature reported FIT [37, 38], first difference is the mode of interaction. FIT-DNA adducts show a positive shift in the peak potential relative to free FIT in CV, favoring intercalative mode of interaction whereas FIS-DNA adducts of FIS presented in Table 1 mostly show negative shifts in the peak potentials relative to free FIS, favoring surface electrostatic mode of interaction of these compounds with DNA. This difference in binding behavior of selenoureas and thioureas may be due to the difference in the reactivities of sulphur and selenium in these two classes of compounds. Because of low ionization potential and high electron density of selenium relative to sulphur it is more susceptible to interact with DNA base pairs [41].

Methyl substitution of phenyl ring attached with ferrocene moiety decreases the magnitude of binding constant by a factor of 10 M^{-1} in general (this article) relative to the scheme in which this ring was not substituted with methyl group in our previous publication [42]. This difference may be because of electron donating nature of methyl group which in turn decreases the electrostatic affinity of FIS with negatively charged phosphate backbone of DNA. Steric factor may also play its role but exact mechanism is not yet clear. In this article 3-chlorophenyl derivative (a16) has shown a binding constant of 2.66 x 10^5 M^{-1} which is ~ 100 times more than 3-chlorophenyl derivative in our previously reported results [42]. Interaction of DNA with drug is very complex and involves different unidentified kinetic parameters because of which structure and activity relation in terms of binding constant, diffusion coefficients and binding site size is not 100% possible.

4.1.2 Free radical scavenging activity

Free radicals are highly reactive and cause diseases such as Alzheimer's disease, myocardial infarction, atherosclerosis, Parkinson's disease, autoimmune diseases, radiation injury, emphysema, sunburns and cancer initiation [23]. In cancer patients free radicals are present at higher concentration than the healthy organisms. It is not yet clear to use the antioxidants during cancer therapy or not. Generally their use is stopped a week before the start of cancer treatment [1]. If an anticancer agent is an efficient free radical scavenger than its importance increases because it can stop cancer initiation as well. This article presents DPPH scavenging activity of synthesized FIS using ascorbic acid as a positive control.

Figure 3 displays the results of DPPH scavenging for synthesized FIS. Generally, ortho substituted derivatives have higher scavenging activities than meta and para substituted derivatives i.e. 2-fluorophenyl derivative has higher scavenging than 3-fluorophenyl and 4-fluorophenyl derivatives and same is the case for methylphenyl derivatives. However this generalization is not followed for other derivatives because there are three different positions in the synthesized FIS which may be involved at the same time in DPPH scavenging i.e. two are the NH groups and the 3rd one is the selenium atom (Figure 4). FIS which showed more than 50% scavenging were evaluated for IC_{50} values which were 152 ± 11.6 µM, 385.1 ± 54.5 µM, 165.6 ± 24.5 µM, 84.3 ± 8.7 µM for a7, a17, a12 and a14 respectively relative to 54.7 ± 2.6 µM of ascorbic acid.

4.1.3 Anti-inflammatory activity

Nitric oxide (NO) is an important signaling molecule but its higher levels are considered to be responsible for ischemic damage, reperfusion injury, obesity, cancer and diabetes [43].

Cancerous cells have been reported to have higher levels of NO [44]. Tumor tissues of male mouse with murine leukemia (Raw 264.7) cells were used to determine the NO inhibition of synthesized FIS using LNMMA (L-N-monomethyl arginine citrate) as a positive control. Figure 5 portraits the NO production inhibition activity of the synthesized FIS which shows that all the compounds displayed the inhibition of NO. Four compounds have better activities than the positive control out of which three are the ortho substituted derivatives. Higher activities of those derivatives which have halogen on ortho position may be due to the formation of an intermediate specie (Figure 6) but higher activities of methyl substituted derivatives is attributed to the higher permeability of these derivatives through the membrane. FIS which have more than 50% inhibition of NO were further evaluated for IC_{50} values which were 10.9 ± 1.4 µM, 35.6 ± 1.0 µM, 24.1 ± 0.4 µM, 14.4 ± 0.7 µM for a7, a17, a12 and a14 respectively relative to the 17.6 ± 5.4 µM of LNMMA.

4.1.4 Enzymatic activities

Cancer initiation in the body is caused by the phase I enzymes (cytochrome P_{450}) because they are responsible for the production of reactive oxygen species (ROS). In response to the higher concentration of ROS, body produces phase II enzymes (glutathione S-transferases (GSTs), UDP-glucuronosyl transferases, and quinone reductases) as a self defense mechanism. Now if an anticancer drug has the ability to inhibit phase I enzyme and induce phase II enzymes in the body it is very useful. In this article we have reported aromatse inhibition (phase I enzyme) and quinone reductase induction (phae II enzyme) activities of the FIS.

4.1.4.1 Aromatase inhibition activity

Breast cancer, ovarian cancer and lungs cancer patients have higher concentrations of estrogen. Biosynthesis of estrogen is controlled by aromatase and it has been reported that aromatse inhibitors are better than tamoxifen for the treatment of breast cancer [45]. Aromatase inhibition activities of the FIS are inferior to the positive control.

4.1.4.2 Quinone reductase (QR) induction activity

Hepa 1c1c7 (murine hepatoma) cells were used for QR activity. For this activity induction ratio of QR1 (IR of QR1) is the specific enzyme induction activity of agent treated cell with reference to DMSO (dimethyl sulfoxide) treated control. Compounds with a QR1 value of 2 or more than 2 are further evaluated for concentration dose (CD) experimentation. CD is that concentration of a chemical which is required to double the QR activity. Figure 7 shows that there are six compounds in the series with QR1 values of more than 2 which were further evaluated for CD values (Figure 8). Quinone reductase induction activities of compounds reported in this article are better than previously reported unsymmetrical diphenyl selenourea and unsymmetrical dimethyl selenourea [23]. Better QR values of compounds with R = methyl, 2-methylphenyl, 3-methylphenyl and 4-methylphenyl are attributed to their easy permeability through cell membrane as they do not contain electronegative substituent which can hinder the permeation. Our hypothesis is further strengthened by highest CD values of methyl substituted derivative (a1). Previously, lower activities of unsymmetric dimethyl selenourea and unsymmetric diphenyl selenourea were attributed to their structural un-similarity with methyl selenol which is considered to be responsible for better chemopreventive action in comparison to the elemental selenium [23]. Our compounds (a1-a17) are not structurally similar to methyl selenol but have shown better activities.

Better performance of Se derivatives (this article) over sulphur derivatives (previous literature) [37, 38] is because of the ability of selenium to attain zwitterionic form via formation of dimeric two cantered three electron bonds which gives selenium an edge over sulphur during different enzymatic studies [23]. These enzymatic activities show that these compounds have the ability to stop the cancer initiation and cancer propagation. In comparison to cis-platin, these compounds are more impressive because cis-platin only kills the cancerous cells but have no effect on cancer initiation and propagation [46].

4.1.5 Activities against the cancer cell lines

Cytotoxic activities have been carried out against five cancerous cell lines namely neuroblastoma cell lines (MYCN and SK-N-SH), lungs cancer cell line (hepa 1c1c7), human cervical carcinoma HeLa cells (ATCC® CCL-2) and breast cancer cell line MCF-7 to further investigate the CP nature of the synthesized FIS.

Neuroblastoma is the cancer of childhood and is extra-cranial malignant in nature [47]. Although the frequency is low in USA (650 cases/year) and UK (100 cases/year) but the problem is serious due to its existence in children. Over expression of a protein NYMc is the reason of this cancer. NYMc is in turn controlled by a gene known as MYCN (neuroblastoma myelocytomatosis). If over expression of NYMc is controlled by controlling or inhibiting MYCN then this cancer can be controlled. Table 2 presents the data of FIS scanned against MYCN. Another neuroblastoma cell line SK-N-SH was also scanned but FIS synthesized are comparatively less active against this cell line. All the compounds have shown activities against MYCN but orthosubstituted compounds (2-fluorophenyl, 2-chlorophenyl, 2-methylphenyl) are the most active and these results are in accordance with our previously published findings [8].

Exact reason for this higher activity is not known to us but these ortho substituted derivatives were the most active against nitrite inhibition as well. We believe that FIS synthesized show higher activity at lower nitrite concentrations but confirmation to this hypothesis requires more work in future.

Liver cancer is the 5th most diagnosed cancer of the world and the activities of FIS against liver cancer cell line hepa1c1c7 have been reported in Table 2. Our synthesized compounds are not much active against this cell line and show 25-30% cell killings.

Breast cancer is 22.7% of all the cancers in the world and in 2008 13.7% of all the cancer deaths were because of this cancer [48]. Activity of FIS against MCF-7 has been presented in Table 2 and once again orthosubstituted (2-chlorophenyl, 2-fluorophenyl) derivatives are the most active but other derivatives have also shown their activities. However highest activity was observed against human cervical carcinoma HeLa cells (ATCC® CCL-2) against which more than 90% cell killing was observed (Table 2).

Conclusion

Chemopreventive nature of ferrocene incorporated selenoureas (FIS) against cancer initiation, cancer propagation and cancer termination has been reported. It was found that FIS are good DPPH (2,2-diphenyl-1-picrylhydrazyl) scavengers, nitrite inhibitors, phase I enzyme (aromatase) inhibitors, phase II enzyme (quinone reductase) inducers and are active against neuroblastoma cell lines (MYCN2 and SK-N-SH), lungs cancer cell line (hepa 1c1c7), human cervical carcinoma HeLa cells (ATCC® CCL-2) and breast cancer cell line MCF-7. If we compare the biological applications of FIS (a1-a17), difference in activities can be attributed to the different R groups in these compounds. Orhto substitued derivatives have shown higher activities possibly due to their better interaction with nitrite chemically. Nitrite levels are high in cancerous cells

and we believe that when FIS interact with nitrite their concentration decreases and at these lower concentrations of nitrite, FIS perform well against cancerous cells.

Acknowledgements

We are thankful to Higher Education Commission Islamabad, Pakistan for financial support.

References

[1] A. Tabassum, R.G. Bristow, V. Venkateswaran, Ingestion of selenium and other antioxidants during prostate cancer radiotherapy: A good thing?, Cancer Treat. Rev., 36 (2010) 230-234.
[2] K.I. Block, A.C. Koch, M.N. Mead, P.K. Tothy, R.A. Newman, C. Gyllenhaal, Impact of antioxidant supplementation on chemotherapeutic efficacy: a systematic review of the evidence from randomized controlled trials, Cancer Treat. Rev., 33 (2007) 407-418.
[3] G. Mugesh, W.-W. du Mont, H. Sies, Chemistry of biologically important synthetic organoselenium compounds, Chem. Rev., 101 (2001) 2125-2180.
[4] R.A. Hussain, A. Badshah, M. Sohail, B. Lal, K. Akbar, Synthesis, chemical characterization, DNA binding and antioxidant studies of ferrocene incorporated selenoure, J. Mol. Struct., 1048 (2013) 367-374.
[5] R.A. Hussain, A. Badshah, M.N. Tahir, T.U. Hassan, A. Bano, Synthesis, Chemical Characterization, DNA Binding, Antioxidant, Antibacterial, and Antifungal Activities of Ferrocence Incorporated Selenoureas, J. Biochem. Mol. Toxicol., 28 (2014) 60-68.
[6] R.A. Hussain, A. Badshah, M.N. Tahir, B. Lal, I.A. Khan, Synthesis, chemical characterisation, and DNA binding studies of ferrocene-incorporated selenoureas, Aust. J. Chem., 66 (2013) 626-634.
[7] R.A. Hussain, A. Badshash, M. Sohail, B. Lal, A.A. Altaf, Synthesis, chemical characterization, DNA interaction and antioxidant studies of ortho, meta and para fluoro substituted ferrocene incorporated selenoureas, Inorg. Chim. Acta, 402 (2013) 133-139.
[8] R.A. Hussain, A. Badshah, J.M. Pezzuto, N. Ahmed, T.P. Kondratyuk, E.-J. Park, Ferrocene incorporated selenoureas as anticancer agents, J. Photochem. Photobiol. B, 148 (2015) 197-208.
[9] B. Mishra, P.A. Hassan, K.I. Priyadarsini, H. Mohan, Reactions of Biological Oxidants with Selenourea: Formation of Redox Active Nanoselenium, J. Phys. Chem. B, 109 (2005) 12718-12723.
[10] D. Desai, S.V. Madhunapantula, K. Gowdahalli, A. Sharma, R. Chandagaludoreswamy, K. El-Bayoumy, G.P. Robertson, S. Amin, Synthesis and characterization of a novel iNOS/Akt inhibitor Se,Se'-1,4-phenylenebis(1,2-ethanediyl)bisisoselenourea (PBISe)—against colon cancer, Bioorg. Med. Chem. Lett., 20 (2010) 2038-2043.
[11] H. Xiao, K.L. Parkin, Induction of Phase II Enzyme Activity by Various Selenium Compounds, Nutr. Cancer, 55 (2006) 210-223.
[12] V. Venkateswaran, N.E. Fleshner, L.H. Klotz, Modulation of cell proliferation and cell cycle regulators by vitamin E in human prostate carcinoma cell lines, The Journal of urology, 168 (2002) 1578-1582.
[13] J. Ni, M. Chen, Y. Zhang, R. Li, J. Huang, S. Yeh, Vitamin E succinate inhibits human prostate cancer cell growth via modulating cell cycle regulatory machinery, Biochemical and Biophysical Research Communications, 300 (2003) 357-363.
[14] A. Nguyen, S. Top, A. Vessières, P. Pigeon, M. Huché, E.A. Hillard, G. Jaouen, Organometallic analogues of tamoxifen: Effect of the amino side-chain replacement by a carbonyl ferrocenyl moiety in hydroxytamoxifen, Journal of Organometallic Chemistry, 692 (2007) 1219-1225.
[15] S. Knauer, B. Biersack, M. Zoldakova, K. Effenberger, W. Milius, R. Schobert, Melanoma-specific ferrocene esters of the fungal cytotoxin illudin M, Anti-Cancer Drugs, 20 (2009) 676-681.
[16] A.P. Ferreira, J.L.F. da Silva, M.T. Duarte, M.F.M. Da Piedade, M.P. Robalo, S.G. Harjivan, C. Marzano, V. Gandin, M.M. Marques, Synthesis and characterization of new organometallic benzo [b] thiophene derivatives with potential antitumor properties, Organometallics, 28 (2009) 5412-5423.
[17] E.A. Hillard, A. Vessières, G. Jaouen, Ferrocene functionalized endocrine modulators as anticancer agents, in: Med. Organomet. Chem., Springer, 2010, pp. 81-117.

[18] O. Payen, S. Top, A. Vessières, E. Brulé, M.-A. Plamont, M. J. McGlinchey, H. Müller-Bunz, G. Jaouen, Synthesis and Structure–Activity Relationships of the First Ferrocenyl-Aryl-Hydantoin Derivatives of the Nonsteroidal Antiandrogen Nilutamide, J. Med. Chem., 51 (2008) 1791-1799.
[19] S. Top, B. Dauer, J. Vaissermann, G. Jaouen, Facile route to ferrocifen, 1-[4-(2-dimethylaminoethoxy)]-1-(phenyl-2-ferrocenyl-but-1-ene), first organometallic analogue of tamoxifen, by the McMurry reaction, J. Organomet. Chem., 541 (1997) 355-361.
[20] S. Top, J. Tang, A. Vessières, D. Carrez, C. Provot, G. Jaouen, Ferrocenyl hydroxytamoxifen: a prototype for a new range of oestradiol receptor site-directed cytotoxics, Chem. Commun., (1996) 955-956.
[21] S. Top, C. Thibaudeau, A. Vessieres, E. Brulé, F. Le Bideau, J.-M. Joerger, M.-A. Plamont, S. Samreth, A. Edgar, J. Marrot, Synthesis and structure activity relationship of organometallic steroidal androgen derivatives, Organometallics, 28 (2009) 1414-1424.
[22] S. Top, A. Vessières, G. Leclercq, J. Quivy, J. Tang, J. Vaissermann, M. Huché, G. Jaouen, Synthesis, Biochemical Properties and Molecular Modelling Studies of Organometallic Specific Estrogen Receptor Modulators (SERMs), the Ferrocifens and Hydroxyferrocifens: Evidence for an Antiproliferative Effect of Hydroxyferrocifens on both Hormone-Dependent and Hormone-Independent Breast Cancer Cell Lines, Chem. Eur. J., 9 (2003) 5223-5236.
[23] R.A. Hussain, A. Badshah, A. Shah, Synthesis and biological applications of selenoureas, Appl. Organomet. Chem., 28 (2014) 61-73.
[24] Q. Feng, N.-Q. Li, Y.-Y. Jiang, Electrochemical studies of porphyrin interacting with DNA and determination of DNA, Anal. Chim. Acta, 344 (1997) 97-104.
[25] M. Aslanoglu, G. Ayne, Voltammetric studies of the interaction of quinacrine with DNA, Anal. Bioanal. Chem., 380 (2004) 658-663.
[26] A. Shah, R. Qureshi, N.K. Janjua, S. Haque, S. Ahmad, Electrochemical and Spectroscopic Investigations of Protonated Ferrocene-DNA Intercalation, Anal. Sci., 24 (2008) 1437-1441.
[27] A. Shah, M. Zaheer, R. Qureshi, Z. Akhter, M. Faizan Nazar, Voltammetric and spectroscopic investigations of 4-nitrophenylferrocene interacting with DNA, Spectrochem. Acta, 75 (2010) 1082-1087.
[28] I.-u.-. Haq, B. Mirza, T.P. Kondratyuk, E.-J. Park, B.E. Burns, L.E. Marler, J.M. Pezzuto, Preliminary evaluation for cancer chemopreventive and cytotoxic potential of naturally growing ethnobotanically selected plants of Pakistan, Pharm. Biol., 51 (2013) 316-328.
[29] L.L. Song, J.W. Kosmeder, S.K. Lee, C. Gerhäuser, D. Lantvit, R.C. Moon, R.M. Moriarty, J.M. Pezzuto, Cancer chemopreventive activity mediated by 4'-bromoflavone, a potent inducer of phase II detoxification enzymes, Cancer Res., 59 (1999) 578-585.
[30] B.-N. Su, J.-Q. Gu, Y.-H. Kang, E.-J. Park, J.M. Pezzuto, A.D. Kinghorn, Induction of the phase II enzyme, quinone reductase, by withanolides and norwithanolides from solanaceous species, Mini-Rev. Org. Chem., 1 (2004) 115-123.
[31] S. Ali, A. Badshah, A.A. Ataf, B. Lal, K.M. Khan, Synthesis of 3-ferrocenylaniline: DNA interaction, antibacterial, and antifungal activity, Med. Chem. Res., 22 (2013) 3154-3159.
[32] R.A. Hussain, A. Badshah, K. Akbar, Comparative DNA binding and antioxidant studies of acetyl and benzoyl substituted ferrocene incorporated selenoureas, Russ. J. Electrochem., 51 (3)198-208 (2014).
[33] R.A. Hussain, A. Badshah, N. Haider, M.D. Khan, B. Lal, Effect of surfactants on the morphology of FeSe films fabricated from a single source precursor by aerosol assisted chemical vapor deposition, J. Chem. Sci., (Firat online 2015).
[34] R.A. Hussain, A. Badshah, S. Marwat, F. Yasmin, M.N. Tahir, Iron selenide nanoparticles coated on carbon nanotubes from single source ferrocene incorporated selenourea precursor for fuel cell and photocatalytic applications, J. Organomet. Chem., 769 (2014) 58-63.

[35] R.A. Hussain, A. Badshah, F. Yasmin, M.D. Khan, M.N. Tahir, Aerosol-Assisted Chemical Vapour Deposition for Iron Selenide Thin Films from Single Source Ferrocene-Incorporated Selenourea Precursor in the Presence of Surfactants, Aust. J. Chem., 68 (2015) 298-306.
[36] R.A. Hussain, A. Badshah, A. Younis, M.D. Khan, J. Akhtar, Iron selenide films by aerosol assisted chemical vapor deposition from single source organometallic precursor in the presence of surfactants, Thin Solid Films, 567 (2014) 58-63.
[37] S. Hussain, A. Badshah, B. Lal, R.A. Hussain, S. Ali, M.N. Tahir, A.A. Altaf, New supramolecular ferrocene incorporated N, N'-disubstituted thioureas: synthesis, characterization, DNA binding, and antioxidant studies, J. Coord. Chem., 67 (2014) 2148-2159.
[38] B. Lal, A. Badshah, A.A. Altaf, M.N. Tahir, S. Ullah, F. Huq, Synthesis, characterization and antitumor activity of new ferrocene incorporated N, N'-disubstituted thioureas, Dalton Trans., 41 (2012) 14643-14650.
[39] M. Waring, Complex formation between ethidium bromide and nucleic acids, J. Mol. Biol. , 13 (1965) 269-282.
[40] N. Shahabadi, S. Kashanian, M. Mahdavi, N. Sourinejad, DNA interaction and DNA cleavage studies of a new platinum (II) complex containing aliphatic and aromatic dinitrogen ligands, Bioinorg. Chem. Appl. , 2011 (2011).
[41] R.A. Hussain, A. Badshah, A. Shah, Synthesis and biological applications of selenoureas, Appl. Organomet. Chem., 2 (2014) 61-73.
[42] R.A. Hussain, A. Badshah, J.M. Pezzuto, N. Ahmed, T.P. Kondratyuk, E.-J. Park, Ferrocene incorporated selenoureas as anticancer agents, J Photochem. Photobiol. B, 148 (2015) 197-208.
[43] F. Aktan, iNOS-mediated nitric oxide production and its regulation, Life sci., 75 (2004) 639-653.
[44] J. Torreilles, Nitric oxide: one of the more conserved and widespread signaling molecules, Front. Biosci. , 6 (2001) D1161-1172.
[45] R. Schneider, A. Barakat, J. Pippen, C. Osborne, Aromatase inhibitors in the treatment of breast cancer in post-menopausal female patients: an update, Breast Cancer: Targets and Therapy, 3 (2011) 113.
[46] M. Cuendet, C.P. Oteham, R.C. Moon, J.M. Pezzuto, Quinone Reductase Induction as a Biomarker for Cancer Chemoprevention⊥, J. Nat. Prod., 69 (2006) 460-463.
[47] A.E. Evans, G.J. D'Angio, J. Randolph, A proposed staging for children with neuroblastoma. Children's cancer study group A, Cancer, 27 (1971) 374-378.
[48] S.H. Giordano, A review of the diagnosis and management of male breast cancer, The Oncologist, 10 (2005) 471-479.

Table 1. DNA binding parameters of ferrocene incorporated selenoureas having below mentioned general structure and different R groups have been mentioned within the table.

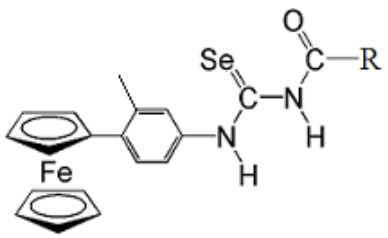

Compounds (R)	K (M^{-1})	D_o (cm^2s^{-1}) Free Drug	D_o (cm^2s^{-1}) Drug-DNA	s (bp)
Methyl	5.48×10^3	3.31×10^{-7}	3.29×10^{-6}	0.05
Phenyl	1.47×10^5	4.41×10^{-7}	4.30×10^{-7}	0.55
4-fluorophenyl	1.03×10^3	1.55×10^{-6}	1.34×10^{-6}	0.41
3-fluorophenyl	1.70×10^3	2.0×10^{-6}	1.0×10^{-6}	0.46
2-fluorophenyl	1.49×10^3	6.42×10^{-5}	4.36×10^{-7}	0.33
2-methylphenyl	3.28×10^5	1.34×10^{-6}	4.68×10^{-7}	0.44
3-methylphenyl	2.08×10^4	2.47×10^{-7}	2.12×10^{-7}	0.04
4-bromophenyl	8.90×10^3	1.38×10^{-6}	6.33×10^{-7}	0.75
3-bromophenyl	4.29×10^3	2.44×10^{-6}	2.22×10^{-6}	0.57
2-bromophenyl	2.62×10^5	2.86×10^{-7}	2.63×10^{-7}	0.75
3-chlorophenyl	2.66×10^5	2.51×10^{-7}	1.51×10^{-7}	1.29

Table 2. Cytotoxicity against different cancerous cell lines of the synthesized FIS.

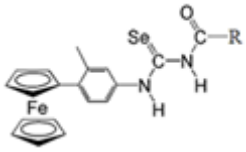 Compound (R)	MYCN-2 % Survival	SK-N-SH % Survival	Hepa 1c1c7 % Survival	MCF-7 % Survival	HeLa % Survival
Methyl	27.9 ± 2.5	70.4 ± 5.0	79.5 ± 2.5	44.7 ± 2.1	32.5 ± 0.6
2-fluorophenyl	11.1 ± 2.6	70.4 ± 6.2	86.7 ± 2.3	37.5 ± 7.4	-
3-fluorophenyl	46.9 ± 3.7	-	76.0 ± 5.3	69.4 ± 7.3	8.0 ± 2.1
4-fluorophenyl	28.5 ± 4.0	85.4 ± 6.2	73.4 ± 2.6	47.2 ± 6.6	-
2-chlorophenyl	17.6 ± 2.2	77.9 ± 3.1	-	46.6 ± 6.4	-
3-chlorophenyl	69.2 ± 0.1	86.3 ± 5.0	75.8 ± 1.7	-	-
4-chlorophenyl	47 ± 0.3	-	69.1 ± 3.7	96.9 ± 1.2	-
3-bromophenyl	65.5 ± 7.7	-	-	75.4 ± 9.0	-
4-bromophenyl	12.1 ± 3.2	66.9 ± 2.5	76.0 ± 1.3	33.1 ± 9.3	5.4 ± 1.6
2-methoxyphenyl	36.4 ± 12.9	98.6 ± 0.4	74.5 ± 2.1	85.2 ± 2.5	9.2 ± 1.1
2-methylphenyl	19 ± 10.3	77.5 ± 0	90.4 ± 1.3	-	-
3-methylphenyl	73.6 ± 23	-	-	85.3 ± 9.4	-
4-methylphenyl	36.6 ± 16.5	77.9 ± 6.8	-	54.5 ± 0.5	10.6 ± 2.4
Aniline	90 ± 6.9	-	-	83.2 ± 2.5	-

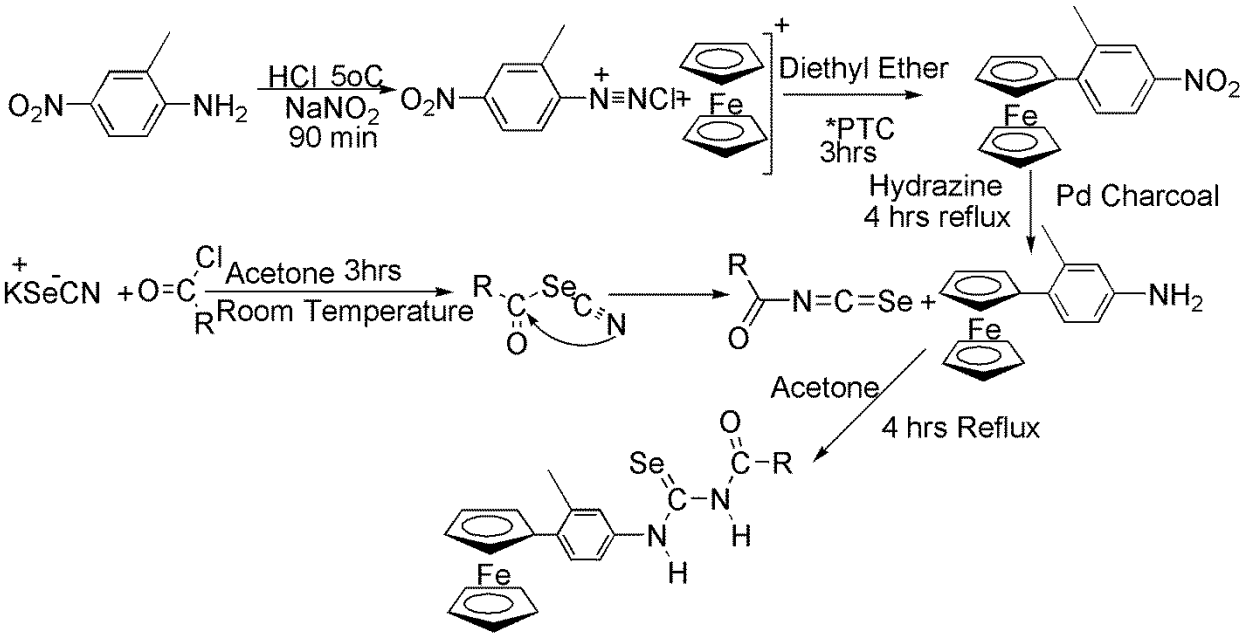

*PTC (Phase transfer catalyst) = hexadecyltrimethyl-ammonium bromide

R = methyl, phenyl, 2-chlorophenyl, 3-chlorophenyl, 4-chlorophenyl, 2-fluorophenyl, 3-fluorophenyl, 4-fluorophenyl, 2-bromophenyl, 3-bromophenyl, 4-bromophenyl, 2-methoxyphenyl, 3-methoxyphenyl, 4-methoxyphenyl, 2-methylphenyl, 3-methylphenyl, 4-methylphenyl

Scheme 1. Synthesis of ferrocene incorporated selenoureas having 3-methyl-4-ferrocenylphenylaniline.

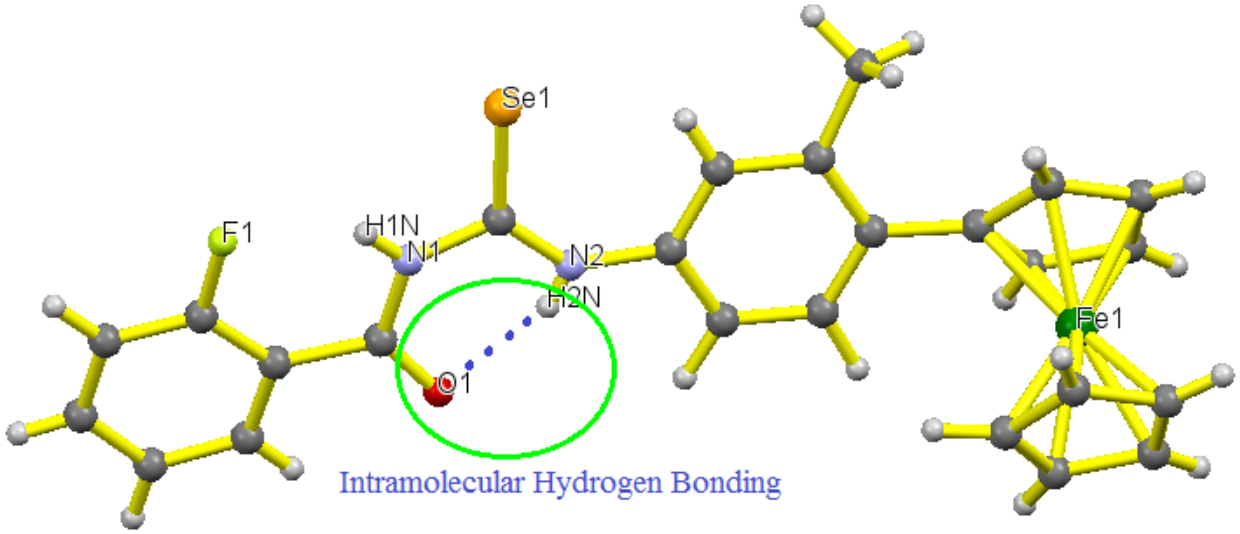

Figure 1. ORTEP diagram for one of the representative compounds namely 1-(2-fluorobenzoyl)-3-(3-methyl-4-ferrocenylphenyl)selenourea showing intramolecular hydrogen bonding [7].

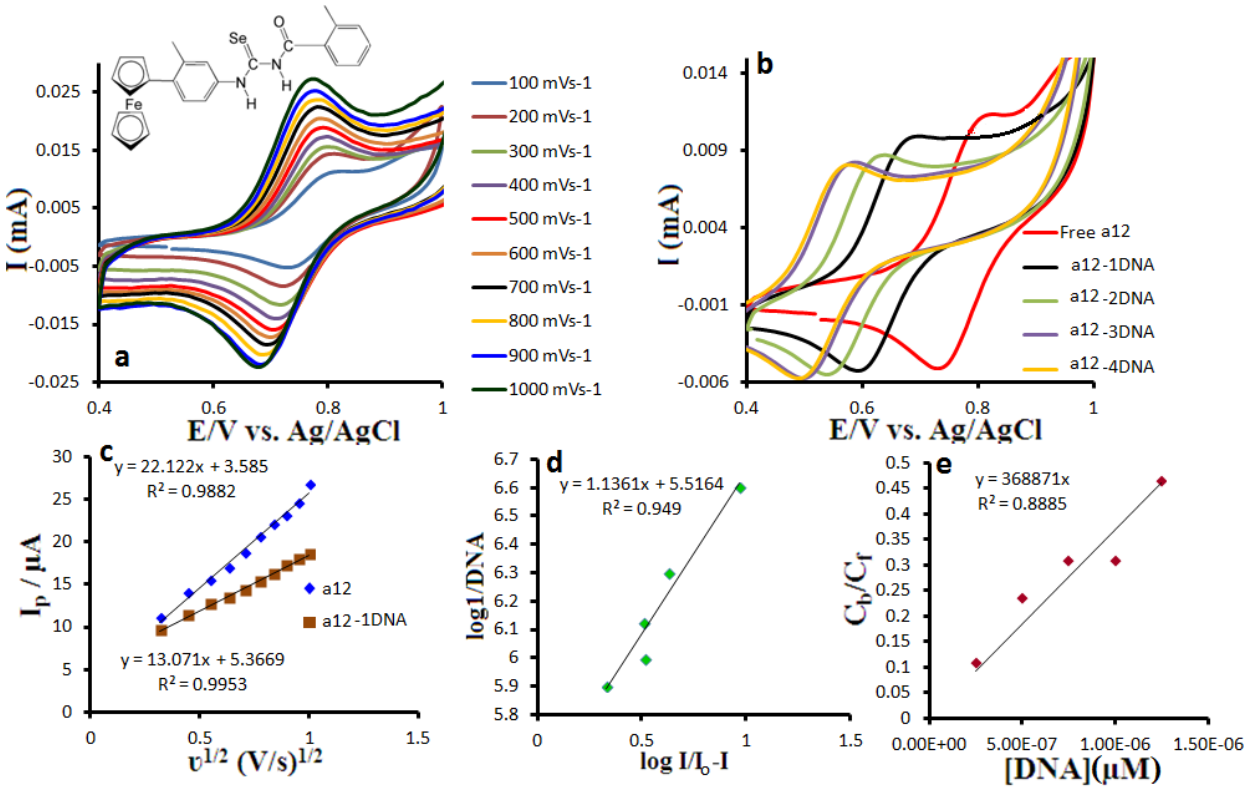

Figure 2. a) Cyclic voltammograms of 1 mM a12 with 1 mL of 1.5 M KCl as a supporting electrolyte at different scan rates. b) Cyclic voltammograms of 1 mM a12 with different DNA concentrations. c) Plots of I vs. $\upsilon^{1/2}$, for the determination of diffusion coefficients of a12 (0 µM DNA) and 2 µM DNA bound a12. d) Plot of log (I/I_o-I) vs. log (1/[DNA]) for determination of binding constant. e) Plot of C_b/C_f vs. [DNA] (µM) for determination of binding site size of 2-8 µM DNA concentrations.

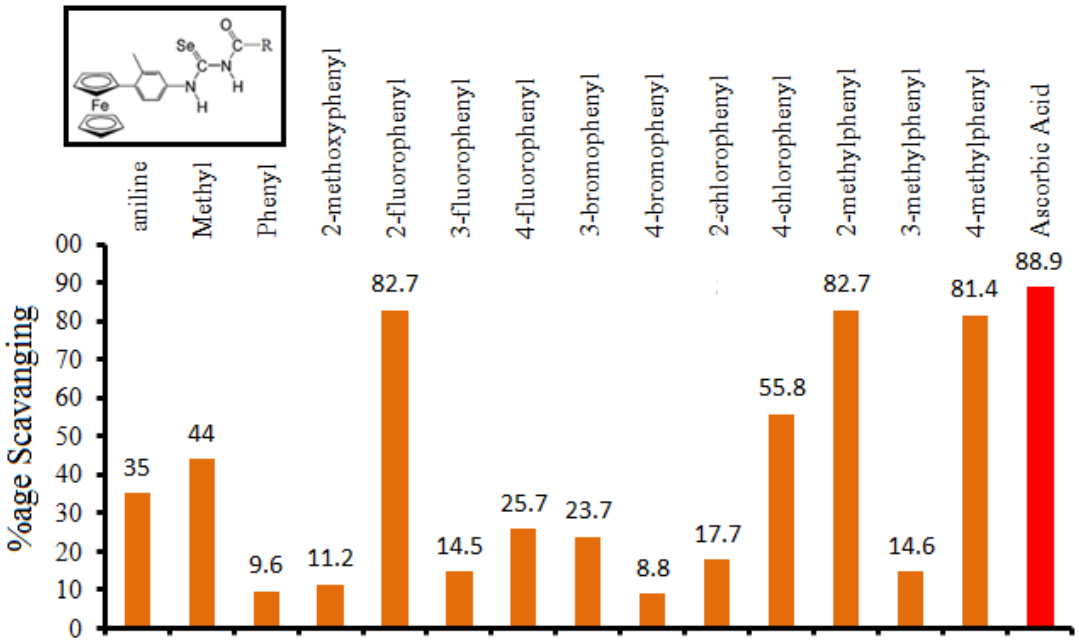

Figure 3. %age DPPH scavenging of synthesized FIS using ascorbic acid as a positive control. General structures for the compounds has been given above the figure whereas R groups are named on the bars.

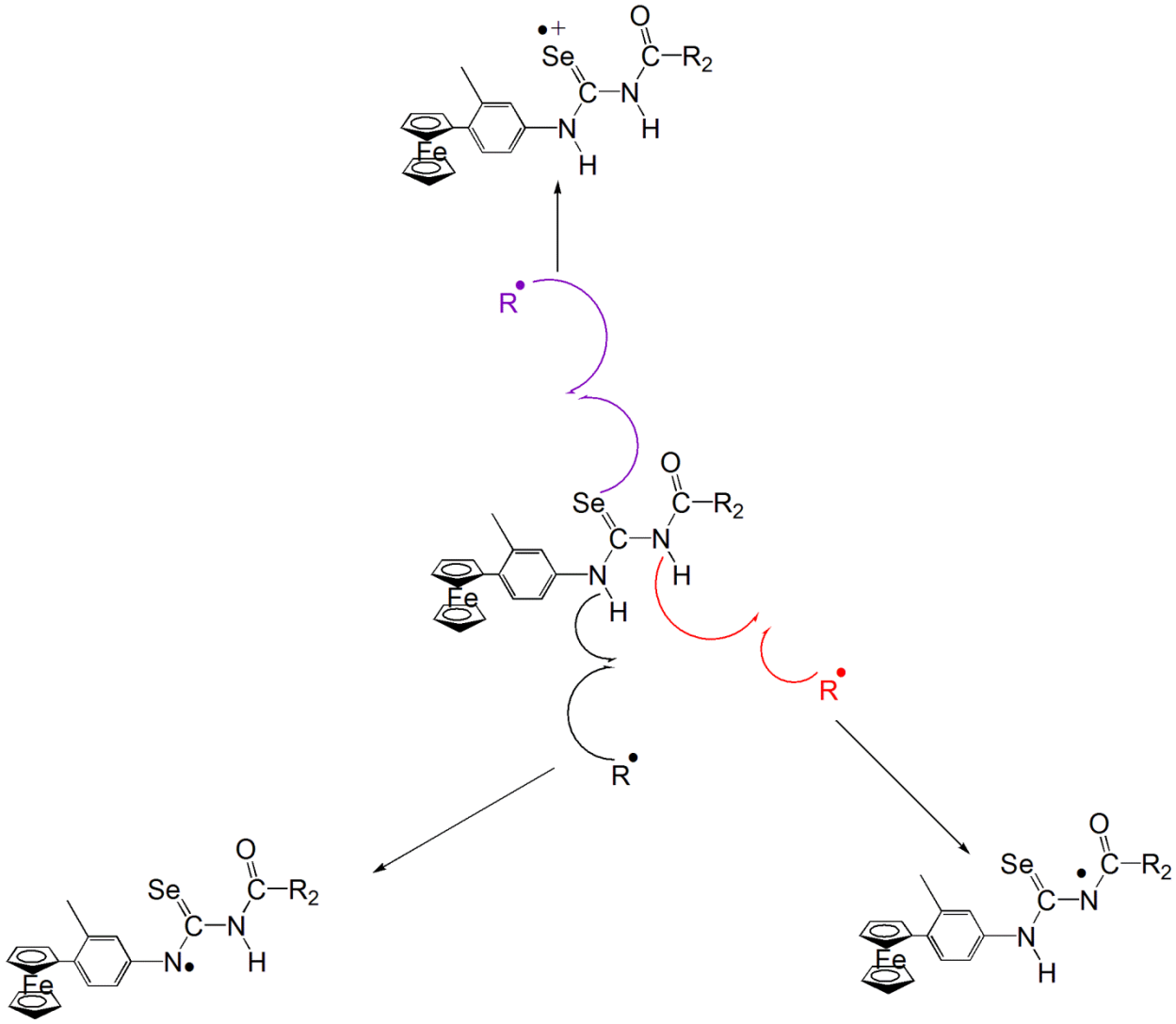

Figure 4. Different possibilities of diphenylpicrylhydrazyl radical scavenging by ferrocene incorporated selenoureas to convert it to diphenylpicrylhydrazine.

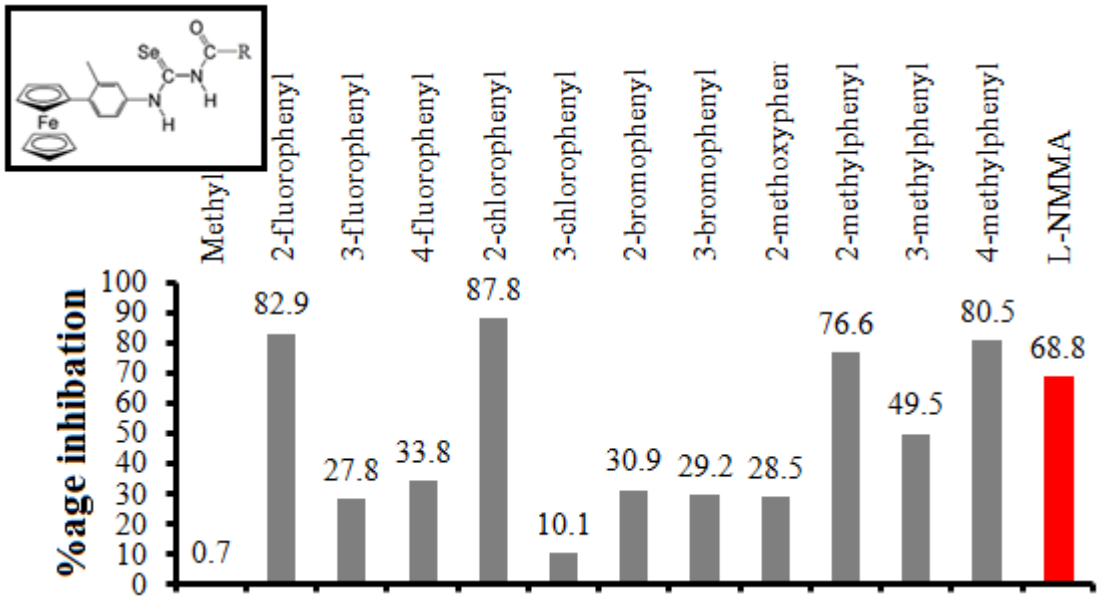

Figure 5. %age NO production inhibition by synthesized FIS using LNMMA as a positive control. General structure for the compounds has been given at the top whereas R groups are embedded within the figure.

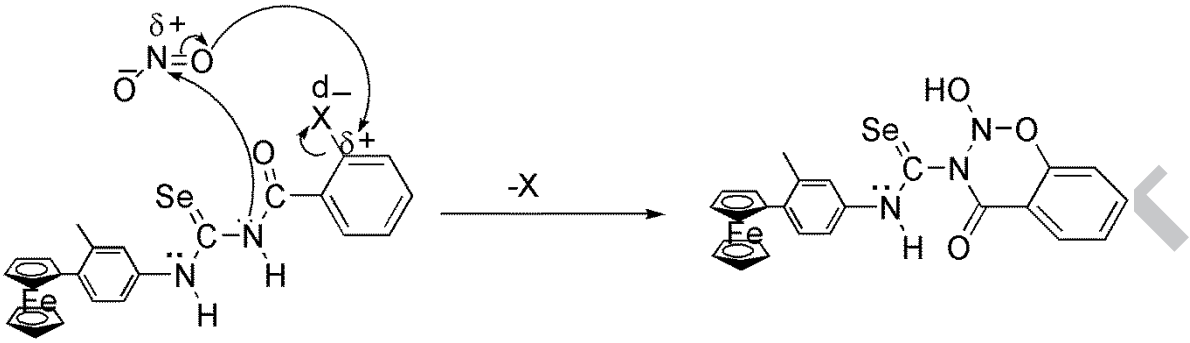

Figure 6. Possible byproduct formed by the interaction of ortho substituted derivatives with NO.

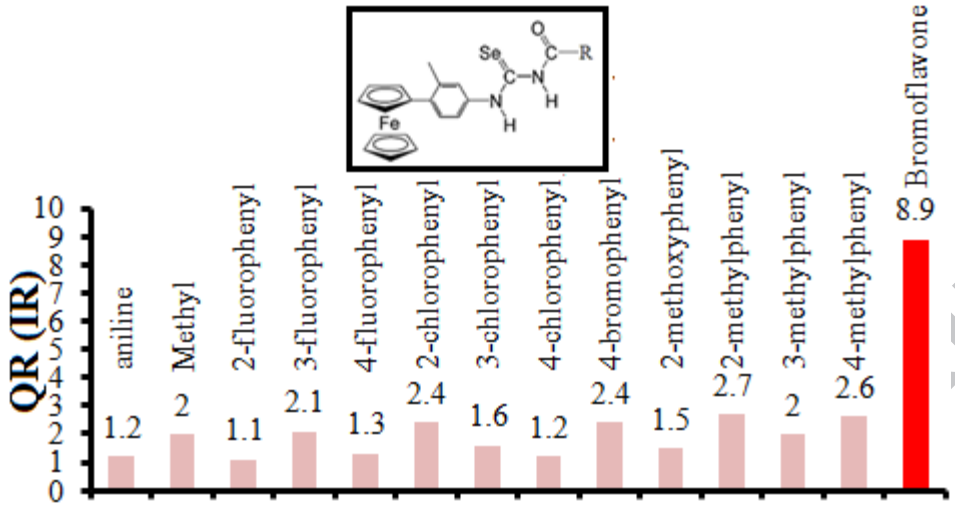

Figure 7. Quinone reductase induction activities of synthesized FIS. General structure of the compounds is presented above the figure whereas R groups are embedded within the figure.

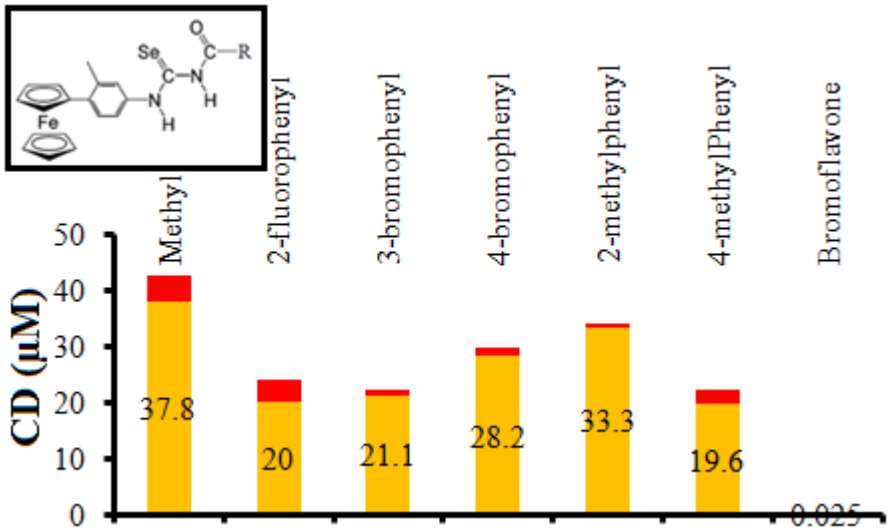

Figure 8. Concentration dose (CD) values of synthesized FIS. General structure of the compounds has been given above the figure whereas R groups are embedded within the figure.

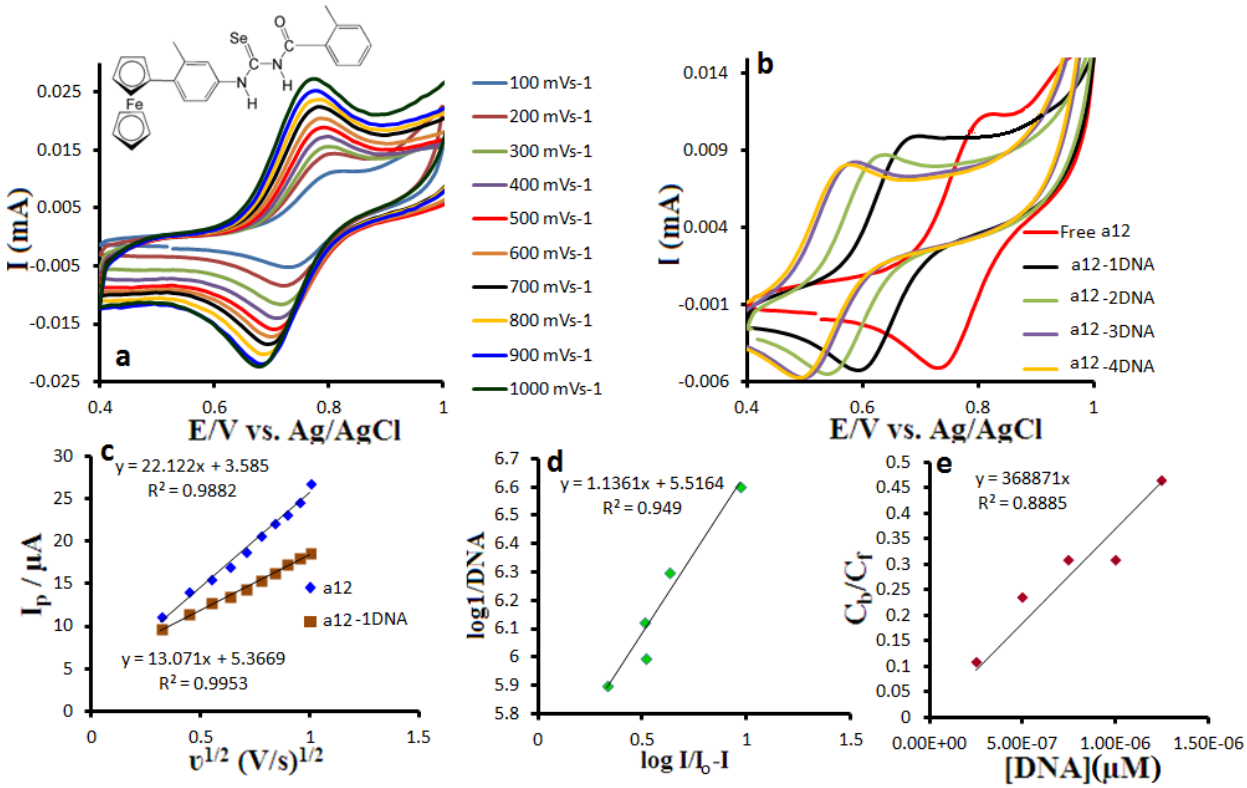

Cyclic voltammograms of 1 mM a12 with 1 mL of 1.5 M KCl as a supporting electrolyte at different scan rates. b) Cyclic voltammograms of 1 mM a12 with different DNA concentrations. c) Plots of I vs. $\upsilon^{1/2}$, for the determination of diffusion coefficients of a12 (0 µM DNA) and 2 µM DNA bound a12. d) Plot of log ($I/I_{\circ}$-I) vs. log (1/[DNA]) for determination of binding constant. e) Plot of C_b/C_f vs. [DNA] (µM) for determination of binding site size of 2-8 µM DNA concentrations.